Chemical Geology xxx (2009) xxx–xxx

Contents lists available at ScienceDirect

Chemical Geology

journal homepage: www.elsevier.com/locate/chemgeo

Geochemical modeling of CO_2 storage in deep reservoirs: The Weyburn Project (Canada) case study

Barbara Cantucci [a,*], Giordano Montegrossi [b], Orlando Vaselli [b,c], Franco Tassi [c], Fedora Quattrocchi [a], Ernie H. Perkins [d]

[a] INGV, Fluid Geochemistry Lab. Rome 1 Section, Via di Vigna Murata 605, Rome, 00143, Italy
[b] CNR - IGG, Institute of Geosciences and Earth Resources, Via La Pira 4, 50121 Florence, Italy
[c] Department of Earth Science, Via La Pira 4, Florence, 50121, Italy
[d] Alberta Research Council, 250 Karl Clark Road, Edmonton, Alberta, Canada T 6N 1E4

ARTICLE INFO

Article history:
Accepted 18 December 2008
Available online xxxx

Keywords:
CO_2 geological storage
EOR Weyburn Oil Field
Brines
Fluid geochemistry
Geochemical modeling

ABSTRACT

Geological storage is presently one of the most promising options for reducing anthropogenic emissions of CO_2. Among the several projects investigating the fate of CO_2 stored at depth, the EnCana's CO_2 injection EOR (*Enhancing Oil Recovery*) project at Weyburn (Saskatchewan, Canada) is the most important oil production development that hosts an international monitoring project. In the Weyburn EOR ~~project~~ CO_2 is used to increase recovery of heavy oil from the Midale Beds, a Mississippian reservoir consisting of shallow marine carbonate, where about 3 billions standard m^3 of supercritical CO_2 have been injected since 2000 with an injection rate of 5000 ton/day.
In this work the available dataset (bulk mineralogy of the reservoir, gas-cap composition and selected pre- and post-CO_2 injection water samples) provided by the *International Energy Agency Weyburn CO_2 Monitoring & Storage Project* has been used in order to:

i) reconstruct the pre-injection reservoir chemical composition (including pH and the boundary conditions at 62 °C and 15 MPa);
ii) assess the evolution of the reservoir subjected to ~~CO_2~~ injection and predict dissolution/precipitation processes of the Weyburn brines over 100 years after injection;
iii) validate the short-term (September 2000–2003) evolution of the in situ reservoir fluids due to the ~~CO_2~~ injection, by comparing the surface analytical data with the composition of the computed depressurized brines.

To achieve these goals the PRHEEQC (V2.14) Software Package was used with both modified thermodynamic database and correction for supercritical CO_2 fugacity. The oil–gas–water interaction and the non-ideality of the gas phase (with exception of CO_2) were not considered in the numerical simulations. Despite intrinsic limitations and uncertainties of geochemical modeling, the main results can be summarized, as follows: 1) the calculated pre-injection chemical composition of the Midale Beds brine is consistent with the analytical data of the waters collected in 2000 (baseline survey), 2) the main reservoir reactions (CO_2 and carbonate dissolution) take place within the first year of simulation, 3) the temporal evolution of the chemical features of the fluids in the Weyburn reservoir suggests that CO_2 can safely be stored by solubility (as $CO_{2(aq)}$) and mineral trapping (via dawsonite precipitation). The short-term validation performed by calculating chemical composition of the reservoir fluids (corrected for surface conditions) after the simulation of 3 years of CO_2 injection is consistent (error ≤5%) with the analytical data of the wellhead water samples collected in 2003, with the exception of Ca and Mg (error >90%), likely due to complexation effect of carboxilic acid.

1. Introduction

The discharge of anthropogenic CO_2 to the atmosphere is considered as a major concern in the control of the global warming (e.g., IPCC, 2005, 2007). A very promising approach to reduce the CO_2 emissions is to capture and dispose this green-house gas (GHG) in suitable deep geological formations (>800 m; e.g., Holloway, 1996; IEA, 2004, 2006), such as saline aquifers, depleted oil and gas fields or unexploited coal beds (e.g., Quattrocchi et al., 2006a). Once injected underground, CO_2 can be retained at depth (Gunter et al., 1993, 2000, 2004), as supercritical fluid (physical trapping), fluid migrating very slowly in an aquifer (hydrodynamic trapping), dissolved $CO_{2(aq)}$ into

* Corresponding author. Tel.: +39 06 51860302; fax: +39 06 51860507.
E-mail address: barbara.cantucci@ingv.it (B. Cantucci).

0009-2541/$ – see front matter © 2009 Elsevier B.V. All rights reserved.
doi:10.1016/j.chemgeo.2008.12.029

Please cite this article as: Cantucci, B., et al., Geochemical modeling of CO_2 storage in deep reservoirs: The Weyburn Project (Canada) case study, Chemical Geology (2009), doi:10.1016/j.chemgeo.2008.12.029

groundwater (solubility trapping), and newly-formed carbonates (mineral trapping). Among these sequestration processes, mineral trapping is likely the most stable (e.g., Gunter et al., 1993, 1997).

The appealing concept that CO_2 could permanently be sequestered underground has favored several experimental and modeling studies. Whatever the trapping process of CO_2, risks of reservoir to surface CO_2 leakage and seepage have to be carefully evaluated (e.g., Pruess and García, 2002; Rutqvist and Tsang, 2002; Damen et al., 2006; Jones et al., 2006; Voltattorni et al., 2006).

The geochemical monitoring of deep fluids is a routine procedure to investigate variations in the fluid composition caused by CO_2 injection and water–rock interactions, and to track the fate of the injected CO_2 plume. Furthermore, the geochemical results are used to develop numerical modeling of deep geochemical processes to: *i)* evaluate theoretical reservoir equilibrium conditions among the several phases (through thermodynamic database, saturation indexes, activities and speciation calculations of liquid phase) and *ii)* reconstruct physico-chemical variations of the different phases at non-equilibrium conditions on the basis of kinetically-controlled reactions (e.g., Marini, 2007).

Generally speaking, owing to the great depth (>800 m) at which the potential CO_2 storage reservoirs are located, the fluid sampling mostly takes place at the wellhead rather than at down-hole (e.g., "Schlumberger" and U-tube technology; Freifeld et al., 2005; Freifeld and Trautz, 2006). Unfortunately, the surface analytical data do not often reflect the reservoir conditions (temperature, pressure, pH and chemical–physical boundary conditions). As the fluid moves from the reservoir to the wellhead, both pressure and temperature decrease. Part of the fluid constituents is lost as gas phase, causing both disequilibrium among the present phases and changes in the fluid chemistry (e.g., Kharaka and Hanor, 2004; Quattrocchi et al., 2006b). Several procedures allow to reconstruct deep fluid composition (e.g., Bazin et al., 1997; Palandri and Reed, 2001; Marini et al., 2003), although their application is usually restricted to geothermal reservoirs (temperatures >100 °C). In these environments pressure can be parameterized as a function of temperature rather than an independent variable, being the pressure fixed at 0.1 MPa for 0–100 °C and following the steam/liquid water equilibrium curve at higher temperatures (100–300 °C; Wolery, 1992). The steam/liquid water curve can be reproduced at laboratory conditions and used to calculate the thermodynamic parameters. For example, Marini et al. (2003) reconstructed the reservoir composition (250 °C and 3 MPa) of geothermal fluids discharged at Miravalles volcano (Costa Rica) highlighting significant compositional variation (about 27%) between the fluids sampled at the wellhead and those computed from the fluids of the reservoir.

Conversely, sedimentary basins suitable for CO_2 geological storage (e.g., oil field pool, saline aquifers) are characterized by low temperature (30–70 °C) and relatively high pressure (>5 MPa). As a consequence, independent thermodynamic parameters cannot be calculated through steam/liquid water curve. Palandri and Reed (2001) approached the problem by assuming a thermodynamic equilibrium between formation waters and reservoir minerals, although their procedure did not take into account the influence of free and/or dissolved gas phases (with exception of CO_2) on chemical composition of the aqueous solution.

In this framework, the main goal of this work is to propose a geochemical model for the hosting aquifers of the Weyburn Oil Field (Canada), where anthropogenic CO_2 is injected since 2000, in order to *i)* reconstruct the pre-injection reservoir chemical composition of the two reservoirs (Marly and Vuggy) where CO_2 is stored by using the geochemical data obtained at the wellhead and provided by the *International Energy Agency Weyburn CO2 Monitoring & Storage Project*, *ii)* assess the (kinetic) evolution of the system during the CO_2 injection and quantify the geochemical trapping mechanisms over 100 years after injection, *iii)* validate the simulated short-term (3 years) evolution of the reservoir during the CO_2 injection by comparison the simulated data with those measured at the wellhead.

2. The Weyburn Oil Field

The Weyburn Oil Field (hereafter WOF) is located in the Prairie Province of Saskatchewan (Western Canada) in the Midale Beds of the Mississippian Charles Formation. The latter is at the depth of 1300–1500 m (El Sayed et al., 1993) and is divided in the Frobisher Evaporite and the Midale Carbonate. Shallow marine carbonate-evaporitic rocks

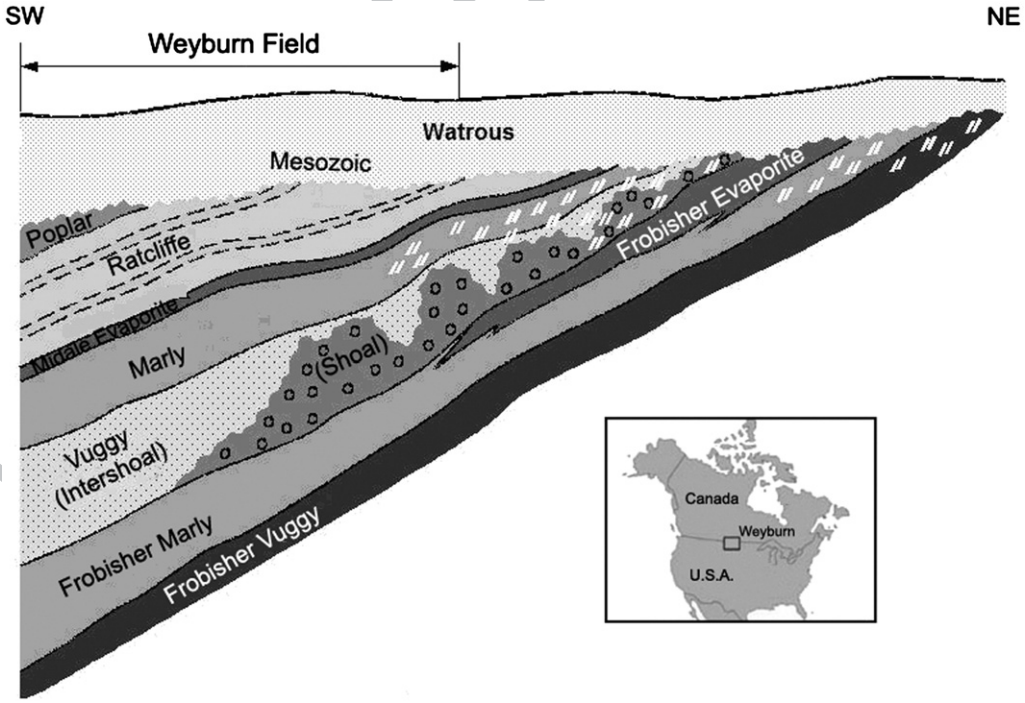

Fig. 1. Location and schematic SW–NE geological cross-section of Midale Beds. The carbonate strata of the oil reservoir are sealed by evaporite beds (Midale Evaporite) and by the Mesozoic Watrous Formation. Modified after Wilson and Monea (2004).

Please cite this article as: Cantucci, B., et al., Geochemical modeling of CO_2 storage in deep reservoirs: The Weyburn Project (Canada) case study, Chemical Geology (2009), doi:10.1016/j.chemgeo.2008.12.029

(Mundy and Roulston, 1998) form the Midale Carbonate where two aquifers, the dolomitic "Marly" and the underlying calcitic "Vuggy", sealed by an anhydrite cap-rock, are hosted (Fig. 1). Pressure and temperature of the reservoirs are 15 MPa and 62 °C, respectively (Rochelle et al., 2002). Detailed geological descriptions of the WOF are reported in Wegelin (1984) and Burrowes (2001).

The oil-rich Midale Beds, discovered in 1954, was exploited by primary depletion until 1964, when secondary oil recovery via water-flooding was implemented (El Sayed et al., 1993). Water-flooding involves re-injection of water less saline than that hosted in the Midale Beds and mainly deriving from the overlying Cretaceous Mannville Aquifer. Presently, more than 3×10^9 standard m^3 of supercritical CO_2, captured from the North Dakota Gasification Power Plant (U.S.A.), are injected (at a rate of 5000 ton/day since September 2000) into the "Phase A1" injection area that includes about 90 oil producers, 30 water injectors and 30 CO_2 injection wells (e.g., Wilson and Monea, 2004).

At the end of the Enhanced Oil Recovery (EOR) operation, in 2025–2030, about 15–20 Mton of anthropogenic CO_2 will be stored in the Mississippian strata with an estimated oil production of 130 million barrels. The Weyburn CO_2-EOR project is the focal point of a multi-disciplinary IEA-EU research program mainly devoted to investigate the fate of CO_2 once injected by using a wide range of monitoring techniques. An exhaustive summary of the specific aspects of this project is reported in Wilson and Monea (2004).

Our geochemical modeling procedure is based on the available dataset provided by the Weyburn Project, which includes: *a)* bulk mineralogy of the Marly and Vuggy reservoirs; *b)* selected pre- and post-CO_2 injection water samples of Midale Beds and *c)* mean gas-cap composition at the wellheads.

2.1. Bulk mineralogy

In this work we adopted a mean mineralogical composition of the Marly and Vuggy reservoirs calculated according to that obtained from 18 core boxes collected from 4 wells located into the injection area (Pearce and Springer, 2001; Springer et al., 2002). The Marly reservoir (from 1 to 11 m thick) is a chalky, microcrystalline dolomite layer with dominantly intercrystalline porosity (26%) (Churcher and Edmunds, 1994). This reservoir is composed by: dolomite (80% by vol.), calcite (14.5%), gypsum (3%), K-feldspar (1.25%), authigenic silica (0.5%), pyrite (0.5%) and clay minerals (0.25%). The Vuggy reservoir (10 to 22 m thick) mainly consists of grainstone and packestone with moldic, intergranular and intercrystalline porosity (Wegelin, 1984), whose mineralogical composition is: calcite (93.5% by vol.), dolomite (3%), anhydrite (2%), authigenic silica (0.5%), pyrite (0.5%) and K-feldspar (0.5%). Average porosity is 14% (Churcher and Edmunds, 1994).

2.2. Aqueous liquid phase

From August 2000 (baseline survey) to September 2004, the University of Calgary and the Alberta Research Council (ARC) jointly with the Italian Institute of Geophysiscs and Volcanology (INGV) have carried out a geochemical monitoring of the pre- and post-CO_2 injection fluids collected at the wellheads. The compositional data of 12 wells (Fig. 2), 7 into the Midale Marly and 5 into the Midale Vuggy, sampled during the baseline (Emberley et al., 2005) and September 2003 (Table 1), are used in the present work. The chemical results of the selected wells (w4, w18, w34, w36–w39 for the Marly and w12, w28, w31, w35 and w41 for the Vuggy) constitute a homogeneous dataset that is to be referred to the 2000–2003 monitoring period.

The WOF baseline fluid chemistry shows a considerable variation in spatial terms across the oil field, likely due to the fact that WOF lies at the boundary between two water types: *i)* a relatively diluted Ca–SO_4 water (Total Dissolved Solids, TDS 10–100 $g\cdot l^{-1}$) and *ii)* a Na–Cl-like brine (TDS 100–300 $g\cdot l^{-1}$) (Bailey et al., 1973; Emberley et al., 2004, 2005). As a consequence, a large variation in salinity, with measured TDS contents varying between 23 and 107 $g\cdot l^{-1}$ (Table 1) is observed. The Marly waters have higher salinity (60–80 $g\cdot l^{-1}$) than those of the Vuggy (38–56 $g\cdot l^{-1}$). This difference is likely due to water-flooding processes that affected the more permeable Vuggy reservoir (Riding and Rochelle, 2004).

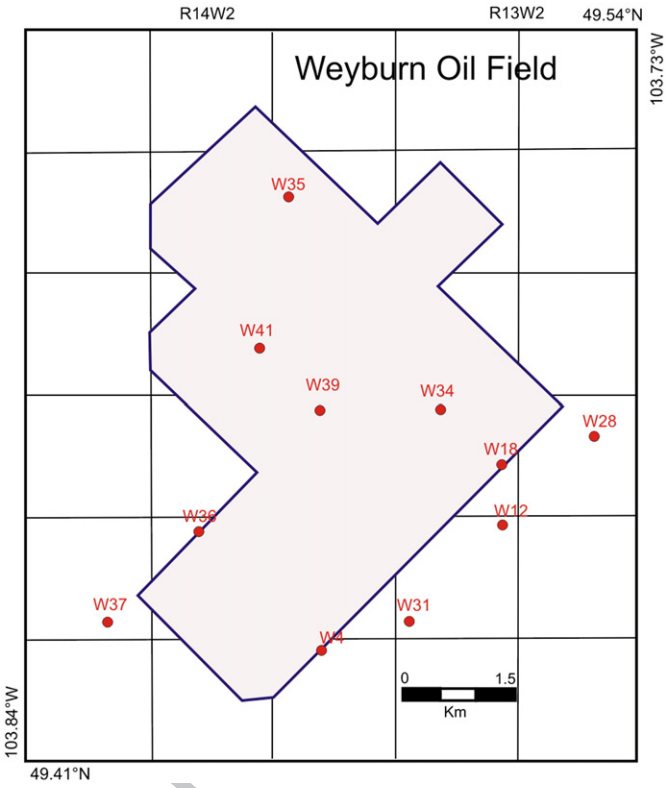

Fig. 2. Geographic location of selected wells for the geochemical model. Wells w4, w18, w34, and w36 to w39 belong to Marly reservoir, while wells w12, w28, w31, w35 and w41 belong to Vuggy reservoir. ~~Numbers in parenthesis are the official location~~ Selected wells have depth ranging from 1400 to 1700 m. Pink area is "Phase A1" injection area. Modified after Emberley et al. (2004). Geographical coordinates system: NAD (North American Data) 83, Zone 13 North.

2.3. Gas phase

In our study the mean gas composition of the Midale Beds reservoir, sampled at wellhead before CO_2 injection (baseline survey) by the University of Calgary, was used. This consists of CH_4 (43.8 mol%), CO_2 (4%), and N_2 (22%). The standard deviations are 12.6, 1.5 and 8.8% for CH_4, CO_2, and N_2, respectively (Emberley et al., 2004). The remaining part of the total gas (31 mol%), composed by ethane, propane, iso and n-butane, iso n-pentane and helium was not considered in the present work. Hydrocarbon components were indeed analyzed by using gas vials partly filled with Cd-acetate in glacial acetic acid (Emberley et al., 2005), likely modifying the original concentrations of the organic species. Analytical data for H_2S were not included because this gas compounds was removed during gas sampling due to safety reasons.

3. Numerical modeling approach

3.1. Simulation method

A numerical model was conceived to assess the short- and long-term geochemical impact of CO_2 injection in WOF system. The model was carried out in five stages (Fig. 3). On the basis of the analytical data of well waters collected at surface in the pre-injection stage (fluids and bulk mineralogy), the chemical composition of fluids at reservoir conditions (62 °C and 15 MPa) (path A) was calculated. Then, we

Please cite this article as: Cantucci, B., et al., Geochemical modeling of CO_2 storage in deep reservoirs: The Weyburn Project (Canada) case study, Chemical Geology (2009), doi:10.1016/j.chemgeo.2008.12.029

Table 1
Analytical chemical composition ($mol \cdot l^{-1}$) of WOF selected wells, sampled at wellheads prior injection of CO_2 (baseline survey, August 2000) by the University of Calgary and ARC (modified after Emberley et al., 2005) and September 2003 after 3 year of CO_2 injection ~~from~~ INGV

Res.	Well	Location	T °C	pH	TDS	Na^+	K^+	Ca^{2+}	Mg^{2+}	HCO_3^-	Cl^-	HS^-	SO_4^{2-}	Li	Fe	Sr	Si
Marly	w 04	14-1 6-14	23.6	6.34	107.81	1.78	1.51×10^{-2}	3.30×10^{-2}	2.83×10^{-2}	8.09×10^{-3}	1.71	3.80×10^{-3}	3.23×10^{-2}	3.51×10^{-3}	4.59×10^{-5}	5.07×10^{-4}	2.45×10^{-4}
Aug. 2000	w 18	b8-18 6-13	21.7	6.45	81.19	1.29	9.30×10^{-3}	3.93×10^{-2}	2.92×10^{-2}	6.49×10^{-3}	1.27	5.26×10^{-3}	3.38×10^{-2}	1.62×10^{-3}	3.05×10^{-5}	4.65×10^{-4}	6.45×10^{-4}
	w 34	d14-18 6-13	19.5	6.31	59.03	0.87	1.01×10^{-2}	3.10×10^{-2}	9.25×10^{-3}	7.17×10^{-3}	0.93	5.72×10^{-3}	3.80×10^{-2}	1.52×10^{-3}	2.68×10^{-5}	9.09×10^{-4}	4.27×10^{-4}
	w 36	d14-11 6-14	37.6	6.50	80.99	1.27	1.31×10^{-2}	4.40×10^{-2}	3.28×10^{-2}	6.38×10^{-3}	1.27	3.23×10^{-3}	3.31×10^{-2}	1.54×10^{-3}	2.71×10^{-5}	4.07×10^{-4}	3.83×10^{-4}
	w 37	2-10 6-14	24.8	6.61	76.55	1.13	6.88×10^{-3}	2.90×10^{-2}	9.09×10^{-3}	9.48×10^{-3}	1.24	6.37×10^{-3}	4.01×10^{-2}	1.50×10^{-3}	1.44×10^{-5}	7.44×10^{-4}	4.43×10^{-4}
	w 38	14-14 6-14	20.9	6.77	67.50	1.08	7.62×10^{-3}	3.51×10^{-2}	1.30×10^{-2}	9.87×10^{-3}	1.03	1.40×10^{-3}	3.53×10^{-2}	1.25×10^{-3}	2.18×10^{-5}	3.43×10^{-4}	2.66×10^{-4}
	w 39	b14-13 6-14	22.3	6.62	72.67	1.18	7.53×10^{-3}	3.50×10^{-2}	1.94×10^{-2}	6.92×10^{-3}	1.11	1.65×10^{-3}	3.60×10^{-2}	1.51×10^{-3}	1.93×10^{-5}	6.06×10^{-4}	3.27×10^{-4}
Vuggy	w 12	d 8-7 6-13	30.2	6.57	34.01	1.21	8.63×10^{-3}	3.90×10^{-2}	6.47×10^{-3}	5.88×10^{-3}	1.19	3.86×10^{-3}	3.74×10^{-2}	1.52×10^{-3}	1.45×10^{-5}	9.59×10^{-4}	3.69×10^{-4}
Aug. 2000	w 28	10-17 6-13	25.2	6.58	92.61	1.49	1.50×10^{-2}	3.76×10^{-2}	3.61×10^{-2}	6.39×10^{-3}	1.44	5.97×10^{-4}	3.95×10^{-2}	1.76×10^{-3}	1.83×10^{-5}	4.48×10^{-4}	4.21×10^{-4}
	w 31	d14-6 6-13	30.3	6.84	88.31	1.29	8.25×10^{-3}	3.43×10^{-2}	5.14×10^{-2}	1.16×10^{-2}	1.46	5.38×10^{-4}	3.17×10^{-2}	2.69×10^{-3}	4.44×10^{-5}	3.62×10^{-4}	4.90×10^{-4}
	w 35	12-25 -14	23.0	6.75	23.43	0.65	3.68×10^{-3}	2.81×10^{-2}	8.10×10^{-3}	8.52×10^{-3}	0.68	8.88×10^{-3}	3.85×10^{-2}	5.46×10^{-4}	9.31×10^{-6}	3.58×10^{-4}	6.45×10^{-4}
	w 41	d8-23 6-14	33.5	7.00	67.98	1.08	1.03×10^{-2}	3.40×10^{-2}	2.22×10^{-2}	7.72×10^{-3}	1.04	5.89×10^{-3}	3.46×10^{-2}	1.25×10^{-3}	2.47×10^{-5}	4.46×10^{-4}	4.28×10^{-4}
Marly	w 04	14-1 6-14	23.6	5.52	120.79	1.81	3.09×10^{-2}	3.86×10^{-2}	2.15×10^{-2}	1.50×10^{-2}	2.00	–	4.01×10^{-2}	4.04×10^{-3}	–	3.50×10^{-4}	5.39×10^{-4}
Sept. 2003	w 18	b8-18 6-13	21.7	5.77	79.64	1.19	1.90×10^{-2}	4.76×10^{-2}	1.98×10^{-2}	2.27×10^{-2}	1.25	–	3.51×10^{-2}	2.25×10^{-3}	–	4.87×10^{-4}	5.61×10^{-4}
	w 34	d14-18 6-13	19.5	6.64	84.84	1.12	1.68×10^{-2}	3.94×10^{-2}	1.82×10^{-2}	1.30×10^{-2}	1.21	–	3.82×10^{-2}	2.11×10^{-3}	–	3.47×10^{-4}	4.89×10^{-4}
	w 36	d14-11 6-14	37.6	5.51	53.13	1.20	1.87×10^{-2}	5.16×10^{-2}	2.07×10^{-2}	4.62×10^{-2}	1.33	–	3.55×10^{-2}	2.36×10^{-3}	–	5.33×10^{-4}	5.35×10^{-4}
	w 37	2-10 6-14	24.8	7.08	84.56	1.24	1.94×10^{-2}	3.75×10^{-2}	1.97×10^{-2}	1.73×10^{-2}	1.36	–	4.04×10^{-2}	2.56×10^{-3}	–	3.56×10^{-4}	4.91×10^{-4}
	w 38	14-14 6-14	20.9	6.91	84.41	0.85	1.35×10^{-2}	3.58×10^{-2}	1.70×10^{-2}	2.06×10^{-2}	0.91	–	3.47×10^{-2}	1.53×10^{-3}	–	3.79×10^{-4}	4.70×10^{-4}
	w 39	b14-13 6-14	25.0	6.91	58.98	1.07	1.62×10^{-2}	4.35×10^{-2}	2.05×10^{-2}	2.97×10^{-2}	1.18	–	3.36×10^{-2}	1.94×10^{-3}	–	5.24×10^{-4}	5.74×10^{-4}
Vuggy	w 12	d8-7 6-13	30.2	6.47	84.85	1.25	1.91×10^{-2}	5.01×10^{-2}	2.15×10^{-2}	1.09×10^{-2}	1.36	–	3.81×10^{-2}	2.30×10^{-3}	–	4.10×10^{-4}	6.36×10^{-4}
Sept. 2003	w 28	10-17 6-13	25.2	6.33	83.96	1.28	2.15×10^{-2}	4.25×10^{-2}	1.99×10^{-2}	1.22×10^{-2}	1.33	–	3.53×10^{-2}	2.43×10^{-3}	–	4.60×10^{-4}	5.70×10^{-4}
	w 31	d14-6 6-13	30.3	6.84	80.10	1.69	2.65×10^{-2}	4.35×10^{-2}	2.24×10^{-2}	1.10×10^{-2}	1.94	–	3.75×10^{-2}	3.74×10^{-3}	–	3.57×10^{-4}	5.56×10^{-4}
	w 35	12-25 -14	23.0	6.37	76.08	0.78	9.84×10^{-3}	3.30×10^{-2}	1.71×10^{-2}	1.62×10^{-2}	0.80	–	3.84×10^{-2}	8.08×10^{-4}	–	$4.79\times10^{-4-}$	3.91×10^{-4}
	w 41	d8-23 6-14	25.0	5.92	74.37	1.25	1.77×10^{-2}	5.55×10^{-2}	2.51×10^{-2}	4.05×10^{-2}	1.37	–	3.35×10^{-2}	2.38×10^{-3}	–	4.77×10^{-4}	6.18×10^{-4}

TDS: Total Dissolved Solids ($g \cdot l^{-1}$).

Please cite this article as: Cantucci, B., et al., Geochemical modeling of CO_2 storage in deep reservoirs: The Weyburn Project (Canada) case study, Chemical Geology (2009), doi:10.1016/j.chemgeo.2008.12.029

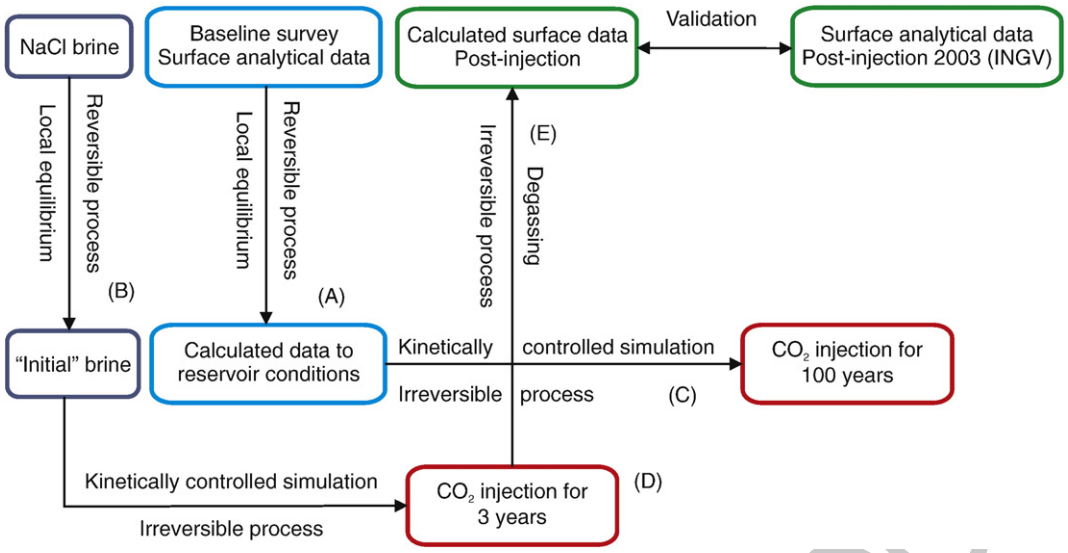

Fig. 3. Schematic sketch of the numerical modeling approach adopted in this study for Marly and Vuggy reservoirs. (A): reconstruction of reservoir chemical composition of formation waters; (B): reconstruction of chemical composition of "initial" brines; (C): evaluation of the geochemical impact of CO_2 injection in WOF system on the long-term (100 years); (D): simulation of CO_2 injection in WOF for 3 years; (E): simulation of fluid uprising process and results of the validation with surface analytical data sampled by INGV in September 2003.

identified the original fluid composition of the Marly and Vuggy reservoirs ("initial" brines) before CO_2 injection (path B). The simulations consider reversible processes where solid, aqueous and gas phases are assumed to be in thermodynamic equilibrium, without taking into account the interaction with the hydrocarbon-rich phase of the WOF. Afterwards, we simulated the CO_2 injection in the WOF system for 100 years (path C) evaluating the efficiency of geochemical trapping mechanism (solubility and mineral trapping). The impact of this irreversible process was calculated via kinetically-controlled reactions. Finally, CO_2 injection in the WOF for 3 years (from 2000 to 2003) was simulated (path D). This irreversible process was also simulated via kinetically-controlled reactions. In order to compare the numerical results with the real analytical data collected by INGV in 2003, the physico-chemical conditions acting on fluids during their flow from the reservoir to the surface were re-constructed (path E). The degassing process needed to compare the simulated results with the analytical data at the third year of injection represents an irreversible step.

To perform our investigations, the PRHEEQC (V2.14; Parkhurst and Appelo, 1999) Software Package, via thermodynamic improvement of the code default database (*phreeqc.dat*) was used in order to obtain a more reliable modeling.

3.2. Reaction rates

Kinetically-controlled reactions can be modeled through the transition state theory (Lasaga, 1984; Lasaga et al., 1994; Steefel and Lasaga, 1994) and expressed by the following general equation:

$$r = kS\left(1-\left(\frac{Q}{K}\right)^{p}\right)^{q} a_{H^+}^{n} \quad (1)$$

where r is the kinetic rate (positive values indicate dissolution and negative values precipitation), k is the kinetic rate constant ($mol \cdot m^{-2} \cdot s^{-1}$), S is the specific reactive surface area ($m^2 \cdot g^{-1}$), Q is the ion activity product,

Table 2
Mineralogical phases considered for the simulations, relative specific surface areas and thermodynamic parameters of the kinetic equations (1)–(5) for modeling the Marly and Vuggy reservoirs

	Log $k_{298.15}$ ($mol \cdot m^{-2} \cdot s^{-1}$)			E_a ($kJ \cdot mol^{-1}$)					Specific surface Area ($m^2 \cdot g^{-1}$)	
	Acid	Neutral	Base	Acid	Neutral	Base	n_1	n_3	Marly	Vuggy
Primary mineral										
K-feldspar	−12.50	~~−15.3~~	−14.20	–	–	–	0.50	0.823	0.175	0.175
Calcite	−0.30	−5.81	−3.48[a]	14.4	23.5	35.4[a]	1.00	1.00[a]	0.034	0.015
Dol.-dis	−3.19	−7.53	−5.11[a]	36.1	52.2	34.8[a]	0.50	0.50[a]	0.105	0.014
Kaolinite	−11.31	−13.18	−17.05	65.9	22.2	17.9	0.77	0.472	2.317	0.015
Chalcedony	–	−12.23	–	–	74.5	–	–	–	0.038	0.015
Pyrite	−7.52[b]	−4.55[b]	–	56.9[b]	56.9[b]	–	−0.50[b]	0.50[c]	0.012	0.008
Secondary mineral										
Gypsum	–	−2.79	–	–	14.3	–	–	–	0.003	0.003
Anhydrite	–	−3.19	–	–	14.3	–	–	–	0.100	0.100
Dawsonite	–	−7.00	–	–	62.8	–	–	–	0.140	0.140
Magnesite	−6.38	−9.34	−5.22	14.4	23.5	62.8	1.00	1.00[a]	0.100	0.100
Muscovite	−11.85	−13.55	−14.55	22.0	22.0	22.0	0.37	0.22	0.106	0.106
Albite	−9.87	−12.04	−16.98	~~65~~	69.8	~~71~~	0.457	0.572	0.115	0.115
Chlorite	−11.11	−12.52	–	88.0	88.0	–	0.50	–	0.113	0.113

Thermodynamic parameters are from Palandri and Kharaka (2004 and references cited therein), with the exception of K-feldspar (Sverdrup, 1990). Rate constants are listed for dissolution. Dol.-dis: disordered dolomite. $k_{298.15}$ is the kinetic constant at 25 °C. E_a is the activation energy and n is the order of the reaction (Eq. (3)).

[a] Reaction order n with respect to $p(CO_2)$.
[b] Reaction order n_1 with respect to H^+ and Fe^{3+}.
[c] Reaction order n_3 with respect to O_2.

Please cite this article as: Cantucci, B., et al., Geochemical modeling of CO_2 storage in deep reservoirs: The Weyburn Project (Canada) case study, Chemical Geology (2009), doi:10.1016/j.chemgeo.2008.12.029

Table 3
Moles per liter of solution of the Marly and Vuggy mineralogical phases used in the in geochemical model

Reservoir	Dol.-dis.	Calcite	Anhydrite	Gypsum	Chalcedony	Pyrite	K-feld.	Kaolinite
	mol	Mol	Mol	Mol	Mol	Mol	mol	Mol
Marly	52.10	8.08	–	0.84	0.45	0.60	0.25	0.05
Vuggy	3.27	87.36	1.52	–	0.75	1.00	0.17	0.00[a]

Dol.-dis: disordered dolomite.
[a] Kaolinite was added as potential secondary mineral in the Vuggy reservoir.

K is the equilibrium constant for a specific mineral–water reaction, p and q are two parameters that depend on the experimental data and they are usually equal to 1, $a^n_{H^+}$ is the aqueous activity of H^+ ion and n is the order of the reaction.

The temperature dependence of the reaction rate constant is expressed by the Arrhenius equation (Lasaga, 1984; Steefel and Lasaga, 1994):

$$k = k_{298.15} \exp\left[\frac{-E_a}{R}\left(\frac{1}{T}-\frac{1}{298.15}\right)\right] \quad (2)$$

where E_a is the activation energy, $k_{298.15}$ is the rate constant at 298.15 K (25 °C), R is the gas constant, T is the absolute temperature (in Kelvin).

In this work the geochemical evolution of the Weyburn system was modeled by using a general equation, which includes terms for reaction mechanisms in pure water (neutral pH), and those depending on H^+ (acid) and OH^- (base) (Lasaga et al., 1994; Palandri and Kharaka, 2004):

$$r = S\left[\begin{array}{l}\left(k_{298.15\text{–acid}} \exp\left[\frac{-E_{a\text{–acid}}}{R}\left(\frac{1}{T}-\frac{1}{298.15}\right)\right] a^{n_1}_{H^+}\right) + \\ + \left(k_{298.15\text{–neutral}} \exp\left[\frac{-E_{a\text{–neutral}}}{R}\left(\frac{1}{T}-\frac{1}{298.15}\right)\right]\right) + \\ + \left(k_{295.15\text{–base}} \exp\left[\frac{-E_{a\text{–base}}}{R}\left(\frac{1}{T}-\frac{1}{298.15}\right)\right] a^{n_3}_{OH^-}\right)\end{array}\right](1-\Omega). \quad (3)$$

The parameter p and q (see Eq. (1)) are set to unit for each mechanism. Additional terms were added to or removed from Eq. (3) to account for other mechanisms (see Table 2) such as those catalyzed by HCO_3^- (especially for the carbonate reaction rate, which depends on HCO_3^- or pCO_2) Fe^{3+} and O_2 (pyrite). Eq. (3) was used for all minerals considered, with exception of pyrite, for which the equation of McKibben and Barnes (1986) was used:

$$r_{pyrite} = S\left[\begin{array}{l}\left(k_{298.15\text{–acid}} \exp\left[\frac{-E_{a\text{–acid}}}{R}\left(\frac{1}{T}-\frac{1}{298.15}\right)\right] a^{n_1}_{H^+} \alpha^{n_2}_{Fe^{3+}}\right) + \\ + \left(k_{298.15\text{–}O_2} \exp\left[\frac{-E_{a\text{–acid}}}{R}\left(\frac{1}{T}-\frac{1}{298.15}\right)\right] \alpha^{n_3}_{O_2}\right)\end{array}\right](1-\Omega) \quad (4)$$

For most minerals precipitation rate data are not available. We can reasonably assume that the precipitation rate of primary and potential secondary minerals is represented by the same kinetic expression as that used for dissolution. The thermodynamic parameters of the kinetic equations for Marly and Vuggy minerals were added to the standard PHREEQC database (Table 2) (Sverdrup, 1990; Palandri and Kharaka, 2004 and reference therein).

The specific reactive surface area is a parameter relatively difficult to be measured or calculated, especially for multi-mineral systems, since only part of the mineral surface is involved in the reaction (e.g., Xu et al., 2007). During kinetic reactions, the specific surface area increases or decreases as the morphology of mineral changes (Wilson, 1975; Grandstaff, 1978; Berner and Holdren, 1979; Berner and Schott, 1982; Velbel, 1984, 1986). This can result in an uncertainty of the modeled results of up to several orders of magnitude (e.g., Gautier et al., 2001). In this study variation of reactive surface area for each mineral was calculated starting from the geometric surface area and the quantity of each mineral, assuming that the reactive surface is proportional to mineral volume fraction. The geometrical features of the surface area was computed by assuming that particles are smooth spheres, through the following general equation:

$$A_{geom} = \frac{6}{\rho d_s}, \quad (5)$$

where A_{geom} is the geometric surface area ($cm^2 \cdot g^{-1}$), ρ is the mineral density ($g \cdot cm^{-3}$) and d_s is the effective spherical diameter of the mineral (cm). Initial values of the geometric surface area for each mineral considered are given in Table 2. The initial surface area of minerals, not present prior to the kinetic simulation, is assigned to be similar to spheres with an average diameter of 0.002 cm for both Marly and Vuggy reservoirs. This value was set on the basis of average grain size analysis of Springer et al. (2002). This assumption is consistent with those values generally assigned to secondary minerals, e.g., spheres with radius of 10^{-5} m (Xu et al., 2004; Gherardi et al., 2007).

3.3. Input data

The mean mineralogical assemblage of the Marly and Vuggy reservoirs (Table 3) was considered as the initial composition for the WOF. Owing the lack of more specific information, chalcedony was used in the modeling as proxy for authigenic silica, which is commonly the controlling SiO_2-phase in sedimentary rocks at low temperature. Kaolinite was used as proxy for clay minerals, whereas dolomite was modeled as disordered dolomite since in the Midale Beds it derives by dolomitization processes (Pearce and Springer, 2001). Kaolinite, not present in the Vuggy reservoir, was added as possible secondary mineral, meaning that this mineral could only be precipitating when supersaturation conditions exist.

Table 4
Enthalpy ($\Delta H°_f$) and free energy of formation ($\Delta G°_f$) of solid species added to the PHREEQC database

Species	$\Delta H°_f$ kJ·mol^{-1}	$\Delta G°_f$ kJ·mol^{-1}	References
Ionic species in aqueous solution[a]			
$Al^{3+}_{(aq)}$	−531.0	−485.0	Hemingway and Robie (1977)
$Mg^{2+}_{(aq)}$	−466.9	−454.8	Parker et al. (1971)
$Ca^{2+}_{(aq)}$	−542.8	−5	Parker et al. (1971)
$H^+_{(aq)}$	0	0	Codata Task Group (1976)
$K^+_{(aq)}$	−252.4	−283.3	Codata Task Group (1976)
$Na^+_{(aq)}$	−240.1	−261.9	Codata Task Group (1976)
$CO_3^{2-}{}_{(aq)}$	−677.1	−527.8	Wagman et al. (1968)
$HCO_3^-{}_{(aq)}$	−692.0	−586.8	Wagman et al. (1968)
$OH^-_{(aq)}$	−230.0	−157.3	Codata Task Group (1976)
$SO_4^{2-}{}_{(aq)}$	−909.3	−744.5	Wagman et al. (1968)
Neutral species[a]			
$H_2O_{(liq)}$	−285.8	−237.1	Codata Task Group (1976)
Solid species			
Dawsonite $NaAlCO_3(OH)_2$	−1963.97	−1785.99	Ferrante et al. (1976)
Dolomite-dis $CaMg(CO_3)_2$	−2324.48	−2161.30	Robie and Hemingway (1977)
Magnesite $MgCO_3$	−1113.28	−1029.48	Robie (1965)

[a] Thermodynamic data from CRC (2001). All values are at standard conditions (25 °C, 0.1 MPa) in an ideal solution 1 M.

Please cite this article as: Cantucci, B., et al., Geochemical modeling of CO_2 storage in deep reservoirs: The Weyburn Project (Canada) case study, Chemical Geology (2009), doi:10.1016/j.chemgeo.2008.12.029

Porosity and bulk density (2.8 g·cm^{-3} and 2.7 g·cm^{-3} for Marly and Vuggy, respectively) of the WOF were used to calculate the water/rock ratio (0.481 and 0.28 for Marly and Vuggy reservoirs, respectively) and the amount of dissolved solids available for reaction in 1 l of water, by assuming that the pore space was water saturated.

Thermodynamic data of *phreeqc.dat* mainly belong to the aqueous model of Nordstrom et al. (1990) and Ball and Nordstrom (1991). However, the thermodynamic properties of some minerals relevant to our model, e.g., disordered dolomite and dawsonite, are not included in the default database *phreeqc.dat*. These data, along with those of magnesite, were added to the original database by using thermodynamic parameters listed in Table 4 that are consistent with those recently published by Palmer et al. (2001) and Bénézeth et al. (2001) (Al^{3+}), Bénézeth et al. (2007) (dawsonite) and Robie and Hemingway (1995) (dolomite).

The primary source for thermodynamic data of aqueous species and minerals was CRC (2001) and Robie et al. (1979). The thermodynamic data were selected in order to maintain an internal coherence with unmodified equilibrium constants in the PHREEQC database. This was achieved by selecting only thermo-chemical measurements and, when possible, values produced by the same research team, due to the high variability of the available data, e.g., solubility product constant (Ksp) of dolomite (Sherman and Barak, 2000). The thermodynamic consistency was checked by using the Born–Haber cycle. Starting from the reference thermodynamic data of ion $\Delta H°_f$ values, mineral formation energies were calculated selecting the data on the basis of the correlation with other possible thermodynamic cycles.

The chemical composition of the 12 wells sampled during the pre-injection baseline survey is reported in Table 1 (Emberley et al., 2005). According to the approach used by Palandri and Reed (2001), Al concentration was estimated by assuming equilibrium with Al-silicates (K-feldspar and/or kaolinite) recognized in the Marly and Vuggy reservoirs, whereas, as already mentioned, organic compounds (e.g., low molecular mass organic acids) were not considered in the geochemical simulation. The mean free gas-cap composition (at wellhead) used for the geochemical simulation of the Weyburn reservoirs is reported in Table 5. The baseline analytical concentration of H_2S was estimated on the basis of aqueous H_2S ($H_2S_{(aq)}$) data measured by INGV in March 2001 (after 6 months of CO_2 injection). The $H_2S_{(aq)}$ concentrations range from 5 to 200 mg·l^{-1}. By assuming a thermodynamic equilibrium between $H_2S_{(aq)}$ and $H_2S_{(g)}$, a mean value of 1.3 mol% of $H_2S_{(g)}$ was calculated by considering the H_2S solubility constant (CRC, 2001). An aliquot of H_2O (0.059 mol%), corresponding to vapor tension calculated at WOF conditions (62 °C and 15 MPa) and an aliquot of $H_{2(g)}$ (0.01 mol%), calculated on the basis of the CH_4–CO_2 redox system in the gas-cap, were added to the gas-cap composition.

Table 5
Wellhead average free gas composition (AC) and multi-component free gas phase composition (MC) used in an irreversible reaction with aqueous phase to increase the total pressure of WOF system from 0.1 to 15 MPa

Gas		AC	MC
	mol%	Partial pressure at 0.1 MPa	Partial pressure (MPa)
CH_4[a]	43.8	0.04380	0.04380
CO_2[a]	4.0	0.00400	–
N_2[a]	22.1	0.02210	0.02210
H_2S	–	0.00130[b]	–
H_2	–	0.00001[c]	0.00001[c]
H_2O	–	0.00059[d]	0.00059[d]
			n_g=186 mol·l^{-1}

[a] Data from Emberley et al. (2004).
[b] estimated value on the basis of average concentration of aqueous H_2S analyzed in the samples collected in March 2001 by INGV.
[c] estimated concentration on the basis of redox potential of H_2S and CH_4 into gas cap.
[d] Water vapor partial pressure at reservoir condition (62 °C, 15 MPa). n_g: numbers of moles of the gas multi-component added to the solution to obtain a total pressure of 15 MPa.

4. Reconstruction of the in-situ reservoir composition (62 °C 15 MPa)

4.1. From baseline pre-injection data to reservoir equilibrium condition (path A)

As previously mentioned, the chemical composition of the WOF deep fluids sampled at wellhead does not reflect the reservoir conditions because temperature and pressure decrease and the gas phase is partially lost as the fluids raise up to the surface. Consequently, a precise knowledge of the reservoir physico-chemical features (T, P, pH, and boundaries conditions) has to be computed, being a necessary pre-requisite for any numerical simulation. In particular, the reconstruction of the chemical composition of the reservoir is the basis to both configure a quantitative model of water–rock interactions and evaluate the CO_2 geochemical impact into the reservoirs.

The pre-injection in-situ reservoir composition was calculated by assuming a thermodynamic equilibrium, at reservoir temperature (62 °C) and pressure (15 MPa), among solid (Table 3), aqueous (Table 1) and gas phases (Table 5). Prior to the CO_2 injection it is indeed reasonable to hypothesize that the fluids in the WOF aquifers, assumed as closed systems, were approaching a chemical equilibrium with their host mineral assemblage. This concept was widely demonstrated for geothermal fluids in equilibrium with alteration minerals at temperatures between 70 and 300 °C (Giggenbach, 1980, 1981; Michard et al., 1981; Arnórsson et al., 1983; Reed and Spycher, 1984; Hull et al., 1987; Giggenbach, 1988; Arnórsson and Andrésdóttir, 1995; Pang and Reed, 1998; Arnórsson, 1999).

The pH values and the chemical composition of the fluid reservoirs were calculated by means of the PHREEQC code, according to the following steps:

1. calculation of the chemical equilibrium for the aqueous, gas and solid phases of the Marly and Vuggy reservoirs at sampling PT conditions (25–30 °C and 0.1 MPa);
2. heat-up of the system from sampling to reservoir temperature (62 °C). This is a routine operation for PHREEQC;
3. simulation of an increase of pressure from wellhead (0.1 MPa) to the reservoir condition (15 MPa) at constant temperature (62 °C). Chemical equilibrium among the various phases was imposed.

In the default thermodynamic data-file, pressure is not an independent variable and the thermodynamic parameters are reported for 0.1 MPa total pressure from 0 to 100 °C. This pressure–temperature grid, however, does not match the *P*–*T* values found in the WOF. As a consequence, the free gas phase pressure was increased to achieve the real pressure of the system. In particular, as the thermodynamic equilibrium between the gas and the aqueous phases is modeled in PHREEQC by assuming an ideal behavior, a multi-component gas phase (Table 5) capable to react irreversibly with the aqueous solution was defined, so that specified amounts of elements are transferred to the aqueous solution during batch reaction. If a gas phase has a fixed volume and temperature, then the pressure in the gas volume will vary with the reaction extent. For WOF, to obtain a total pressure of 15 MPa, 186 mol·l^{-1} of the gas multi-component were added to the solution. This value was computed by considering the amount of gas soluble at the reservoir conditions. The $CO_{2(g)}$ and $H_2S_{(g)}$ contents were not included in batch reaction. By considering the high amount of moles needed to obtain a pressure of 15 MPa, the introduction of these highly reactive species would imply: *i)* a system over-saturated in CO_2 and, *ii)* a high reducing environment able to strongly modify all aqueous phase constituents. Moreover, in the WOF reservoir gas-cap only very small amounts of $CO_{2\,(g)}$ and $H_2S_{\,(g)}$ are likely present, and the baseline analytical data did not show any evidence of CO_2-induced alteration.

Equilibrium reactions were simulated for successive incremental steps (150). For each step, a specific amount of reactant was added to the solution and the resulting system was equilibrated. The results of the previous time step were the starting point of the successive step.

Please cite this article as: Cantucci, B., et al., Geochemical modeling of CO_2 storage in deep reservoirs: The Weyburn Project (Canada) case study, Chemical Geology (2009), doi:10.1016/j.chemgeo.2008.12.029

Table 6
Calculated pre-injection chemical composition (mol·l^{-1}) of selected wells and "initial" waters of WOF at reservoir conditions of 62 °C and 15 MPa

Res.			pH	Na^+	K^+	Ca^{2+}	Mg^{2+}	HCO_3^-	Cl^-	HS^-	SO_4^{2-}	Li	Sr	Si	Al
	Well	Location													
Marly	w 04	14-1 6-14	6.70	1.87	6.40×10^{-2}	9.87×10^{-4}	6.66×10^{-6}	7.33×10^{-3}	1.80	9.86×10^{-2}	4.62×10^{-5}	3.70×10^{-3}	5.35×10^{-4}	3.73×10^{-4}	6.82×10^{-8}
	w 18	b8-18 6-13	6.56	1.33	8.51×10^{-2}	8.60×10^{-3}	3.63×10^{-5}	2.08×10^{-3}	1.30	7.27×10^{-2}	4.43×10^{-5}	1.76×10^{-3}	5.06×10^{-4}	4.63×10^{-4}	6.59×10^{-8}
	w 34	d14-18 6-13	6.78	0.86	5.07×10^{-2}	1.47×10^{-3}	4.48×10^{-6}	1.09×10^{-2}	0.93	1.10×10^{-1}	6.65×10^{-5}	1.52×10^{-3}	9.10×10^{-4}	4.98×10^{-4}	1.12×10^{-7}
	w 36	d14-11 6-14	6.70	1.30	6.21×10^{-2}	3.05×10^{-3}	1.31×10^{-5}	4.20×10^{-3}	1.30	9.52×10^{-2}	2.39×10^{-5}	1.58×10^{-3}	4.17×10^{-4}	4.38×10^{-4}	8.30×10^{-8}
	w 37	2-10 6-14	6.83	1.15	4.61×10^{-2}	1.21×10^{-3}	4.72×10^{-6}	8.84×10^{-3}	1.27	1.25×10^{-1}	6.51×10^{-5}	1.53×10^{-3}	7.58×10^{-4}	4.53×10^{-4}	1.14×10^{-7}
	w 38	14-14 6-14	6.80	1.09	4.91×10^{-2}	1.85×10^{-3}	6.43×10^{-6}	7.14×10^{-3}	1.04	1.11×10^{-1}	4.53×10^{-5}	1.26×10^{-3}	3.46×10^{-4}	4.73×10^{-4}	1.11×10^{-7}
	w 39	b14-13 6-14	6.73	1.33	5.82×10^{-2}	2.57×10^{-3}	1.11×10^{-5}	4.63×10^{-3}	1.30	1.03×10^{-1}	2.85×10^{-5}	1.66×10^{-3}	4.77×10^{-4}	4.37×10^{-4}	8.81×10^{-8}
Vuggy	w 12	d 8-7 6-13	6.69	1.25	6.43×10^{-2}	2.50×10^{-3}	1.05×10^{-5}	5.46×10^{-3}	1.24	1.62×10^{-1}	5.29×10^{-5}	1.58×10^{-3}	9.96×10^{-4}	4.41×10^{-4}	8.09×10^{-8}
	w 28	10-17 6-13	6.62	1.57	7.63×10^{-2}	2.62×10^{-3}	1.43×10^{-5}	4.38×10^{-3}	1.53	1.41×10^{-1}	3.88×10^{-5}	1.86×10^{-3}	4.74×10^{-4}	4.01×10^{-4}	6.26×10^{-8}
	w 31	d14-6 6-13	6.59	1.36	8.07×10^{-2}	3.48×10^{-3}	1.75×10^{-5}	3.88×10^{-3}	1.54	1.32×10^{-1}	3.17×10^{-5}	2.83×10^{-3}	3.82×10^{-4}	4.13×10^{-4}	6.11×10^{-8}
	w 35	12-25 -14	6.75	0.65	5.33×10^{-2}	4.51×10^{-3}	1.21×10^{-5}	4.34×10^{-3}	0.68	1.75×10^{-1}	4.11×10^{-5}	5.47×10^{-3}	3.59×10^{-4}	5.25×10^{-4}	1.10×10^{-7}
	w 41	[illegible]6-14	6.69	1.11	6.31×10^{-2}	4.65×10^{-3}	1.73×10^{-5}	3.36×10^{-3}	1.07	1.60×10^{-1}	3.16×10^{-5}	1.29×10^{-3}	4.59×10^{-4}	4.61×10^{-4}	8.56×10^{-8}
	Initial														
Marly			6.91	1.84	3.88×10^{-2}	1.44×10^{-3}	8.10×10^{-6}	3.89×10^{-3}	1.43	1.37×10^{-1}	3.31×10^{-5}	–	–	3.96×10^{-4}	1.18×10^{-7}
Vuggy			6.76	1.02	5.29×10^{-2}	4.35×10^{-3}	1.40×10^{-5}	3.61×10^{-3}	0.79	1.75×10^{-1}	3.58×10^{-5}	–	–	4.88×10^{-4}	1.06×10^{-7}

In the simulation for reconstructing the chemical conditions of the Marly and Vuggy reservoirs, some conceptualism was applied. Since 1964, the WOF was subjected to water injection as secondary recovery mechanism from the Cretaceous Mannville aquifer (Wilson and Monea, 2004). As no information about the water volume and the injection rate are available, the effects of water-flooding were not considered in this simulation. This introduces large uncertainties in the numerical modeling and can affect the assumption of thermodynamic equilibrium. Furthermore, for the sake of homogeneity of simulation, average composition of the solid phase for the Marly and Vuggy reservoirs was used. The lack of analytical data has not allowed the use of the dissolved organic species, likely present in the WOF system.

The chemical composition variation of the selected waters for the Marly and Vuggy aquifers from the sampling to the computed reservoir conditions is reported in Table 6 and shown in Fig. 4.

Wellhead waters show partial equilibrium with the mineralogical assemblage of the Marly and Vuggy reservoirs and are oversaturated with respect to calcite, disordered dolomite and pyrite, whereas only chalcedony and anhydrite/gypsum are in equilibrium. Owing to initial partial equilibrium between fluids and solid phases of the Marly and Vuggy reservoirs, the equilibrium constrain in batch modeling produced significant variation in the overall chemistry of the aqueous solutions and in the mineralogical assemblage.

From surface to reservoir, pH values for Marly and Vuggy waters slightly increase (from 6.61 to 6.70). As a consequence, the equilibrium batch modeling predicts the precipitation of calcite and dolomite with a decrease of Ca^{2+} and Mg^{2+} concentrations ranging from 3.49×10^{-2} and 2.21×10^{-2} to 3.12×10^{-3} and 1.29×10^{-5} mol·l^{-1}, respectively, while HCO_3^- concentration decrease of about 29% (from 7.88×10^{-3} to 5.55×10^{-3} mol·l^{-1}). Also, a partial dissolution of K-feldspar in both Marly and Vuggy reservoirs and chalcedony precipitation is likely occurring. As a consequence, concentrations of K^+ (from 9.62×10^{-3} to 6.27×10^{-2} mol·l^{-1}) and Al increase of 6 and 28 times (from 3.12×10^{-9} to 8.69×10^{-8} mol·l^{-1}), respectively, while Si concentration does not show significant variations (from 4.24×10^{-4} to 4.48×10^{-4} mol·l^{-1}). Equilibrium batch modeling suggests total dissolution of gypsum and anhydrite, and SO_4^{2-} reduction to HS^-, the former decreasing of 3 orders of magnitude (from 3.59×10^{-2} to 4.30×10^{-5} mol·l^{-1}). Accordingly, pyrite slightly precipitates (2.4×10^{-5} mol·l^{-1}) lowering the concentration of Fe from 2.36×10^{-4} to 6.91×10^{-13} mol·l^{-1}.

Finally, Na^+, Cl^-, Li and Sr concentrations measured at the wellhead do not show significant variations with respect to those of the calculated chemical composition (Fig. 4).

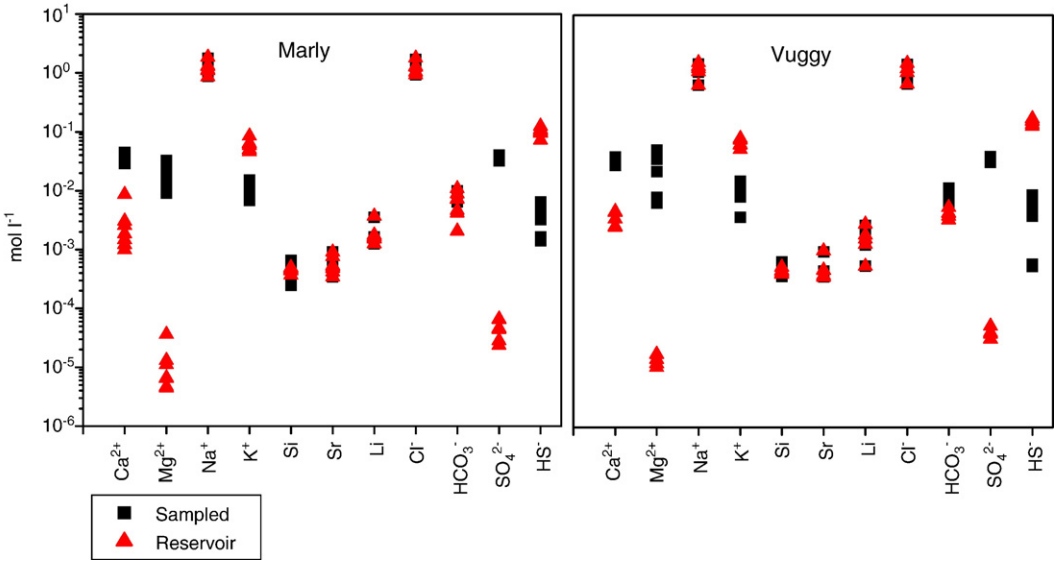

Fig. 4. Comparison between the chemical composition of calculated Marly and Vuggy waters at reservoir conditions (red triangles) (62 °C and 15 MPa) and the analytical pre-injection composition (black squares) of Marly and Vuggy waters. (For interpretation of the references to colour in this figure legend, the reader is referred to the web version of this article.)

Please cite this article as: Cantucci, B., et al., Geochemical modeling of CO_2 storage in deep reservoirs: The Weyburn Project (Canada) case study, Chemical Geology (2009), doi:10.1016/j.chemgeo.2008.12.029

4.2. Reconstruction of the "initial" brine composition (62 °C, 15 MPa) (path B)

Owing to the highly variable salinity of the WOF water composition (TDS 23–107 g·l^{-1}) and the assumptions necessary to model complex systems, the chemical composition calculated at reservoir conditions should be considered with caution. In this contest, for a more correct and careful reconstruction of the reservoir conditions, each well water should have been associated to the solid and gas phase directly in contact with it. However, due the quality of the available dataset (e.g., average composition of mineralogy and gas phase, lack of information about water-flooding), an average composition of formation water for each considered reservoir was assumed as the most appropriate. Therefore, we calculated potential compositions of the pre-injection reservoir aqueous phases ("initial" brine), for the Marly and Vuggy reservoirs, respectively. The so defined "initial" reservoir compositions were obtained by geochemical modeling, assuming equilibrium conditions among: a) the average mineral assemblage of Marly and Vuggy (Table 3), b) a Na–Cl equivalent brine with a Cl/Na ratio similar to that of seawater (Cl/Na = 1.2), and neutral pH (i.e., 7) and c) the mean free gas-cap composition sampled at the wellheads (Table 5). The simulation was carried out by using an approach similar to that previously used to calculate the reservoir chemical composition. The system was heated-up from surface to reservoir temperature (62 °C) and the pressure increase (from 0.1 to 15 MPa) was simulated, defining a multi-component gas phase (Table 5) able to irreversibly react with the aqueous solution. By comparing the chemical compositions of the "initial" brine of Marly and Vuggy (Table 6) with those of the pre-injection water, calculated at reservoir conditions, a good agreement for most analytical species is observed (Fig. 5). The "initial" concentrations of K^+, Ca^{2+}, HCO_3^-, Mg^{2+}, SO_4^{2-} are lower than those calculated at the same reservoir conditions from analytical data (Table 6), reflecting the high variability in salinity of WOF waters. The calculated "initial" pH values are 6.91 and 6.76 for the Marly and Vuggy reservoirs, respectively. These values slightly differ from those calculated at reservoir condition (6.73 and 6.67 for Marly and Vuggy, respectively).

The use of an equivalent-NaCl solution is a classical approach used in many geochemical simulations applied to CO_2 storage (e.g., Gunter et al., 1993, 1997; Xu et al., 2004; Gherardi et al., 2007) where analytical data are lacking. The error induced by this type of approach was estimated by Kervévan et al. (2005) to be less than 5%. In our case, the equivalent-NaCl approximation allows to bypass the uncertainty of more than 36 years of water-flooding in WOF water composition. The reconstruction of "initial" brine compositions is the starting point to assess the geochemical impact and evolution of CO_2 into the oil reservoir vs. time and to quantify water–gas–rock reactions over long time (i.e., 100 years).

5. Temporal evolution of the Weyburn system subjected to CO_2 injection

Modeling the kinetic aspects of water–rock–gas interactions is an indispensable tool when the temporal evolution of a reservoir, undergoing CO_2 injection, is to be assessed. However, some processes involving mineral–brine–CO_2 reactions remain poorly understood. In particular, the dissolution kinetic rate of supercritical CO_2 in saline water is unknown, although several authors (e.g., Gunter et al., 1997; Xu et al., 2003; Gauss et al., 2005; Perez et al., 2006; Marini, 2007; Xu et al., 2007) agree that it may be considered as a kinetically rapid process. In contrast, the rate with which CO_2-rich brine reacts with primary minerals is relatively slow. The most rapidly dissolving minerals are carbonates (with rate constant between 10^{-5} and 10^{-8} mol·m^{-2}·s^{-1}), whereas silicate dissolution (with rate constant between 10^{-9} and 10^{-16} mol·m^{-2}·s^{-1}) can take hundreds of years to attain equilibrium condition (Gunter et al., 2000). On the contrary, chemical equilibrium models can be used only to describe properly reversible and fast reactions only (Marini, 2007). Therefore, calculation of the amount of CO_2 that can geochemically be trapped, only based on equilibrium assumption, may be overestimated after a certain span of time.

5.1. Kinetic simulations at 100 years (path C)

Kinetic simulations of CO_2-rich "initial" Marly and Vuggy waters interacting with the host-rock minerals was performed over 100 years after the injection. Dawsonite, magnesite, chlorite, muscovite, albite, anhydrite (in the Vuggy) and gypsum (in the Marly) were added as potential secondary minerals.

Kinetic simulations for each reservoir were carried out at isothermal conditions of 62 °C, under a CO_2 injection constant pressure of 15 MPa. The CO_2 gas pressure is assumed to be in equilibrium with the solution at all times. The solubility of CO_2 in the aqueous phase depends on pressure, temperature and salinity. At low pressure (atmospheric range) gas species can be considered to behave as an ideal mixture and the fugacity coefficient is assumed equal to 1. At higher temperature and pressure typical of CO_2 deep aquifer injection, the assumption of ideal gas and ideal behavior is not any longer valid, and the fugacity coefficient should be corrected according to the temperature and pressure of the studied system (Spycher and Reed, 1988). Pure CO_2 supercritical fugacity and solubility were computed by means of the thermodynamic model of Duan et al. (1992, 2006) and Duan and Sun (2003). These authors presented an empirical model based on a specific interaction theory for the liquid phase (Pitzer, 1973, 1979) and a highly accurate Equation Of State for the vapour phase (Duan et al., 1992) capable of calculating CO_2 solubility in complex saline aqueous fluids for temperatures from 0 to 260 °C, pressures from 0 to 200 MPa and ionic strengths from 0 to

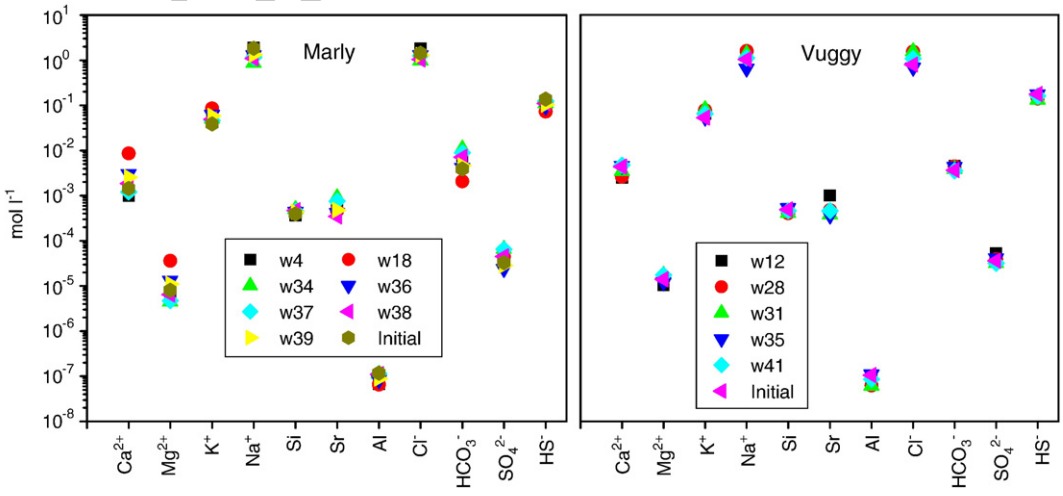

Fig. 5. Comparison between the calculated "initial" brine and the analyzed pre-injection baseline survey data re-calculated to reservoir compositions for the Marly and Vuggy waters.

Please cite this article as: Cantucci, B., et al., Geochemical modeling of CO_2 storage in deep reservoirs: The Weyburn Project (Canada) case study, Chemical Geology (2009), doi:10.1016/j.chemgeo.2008.12.029

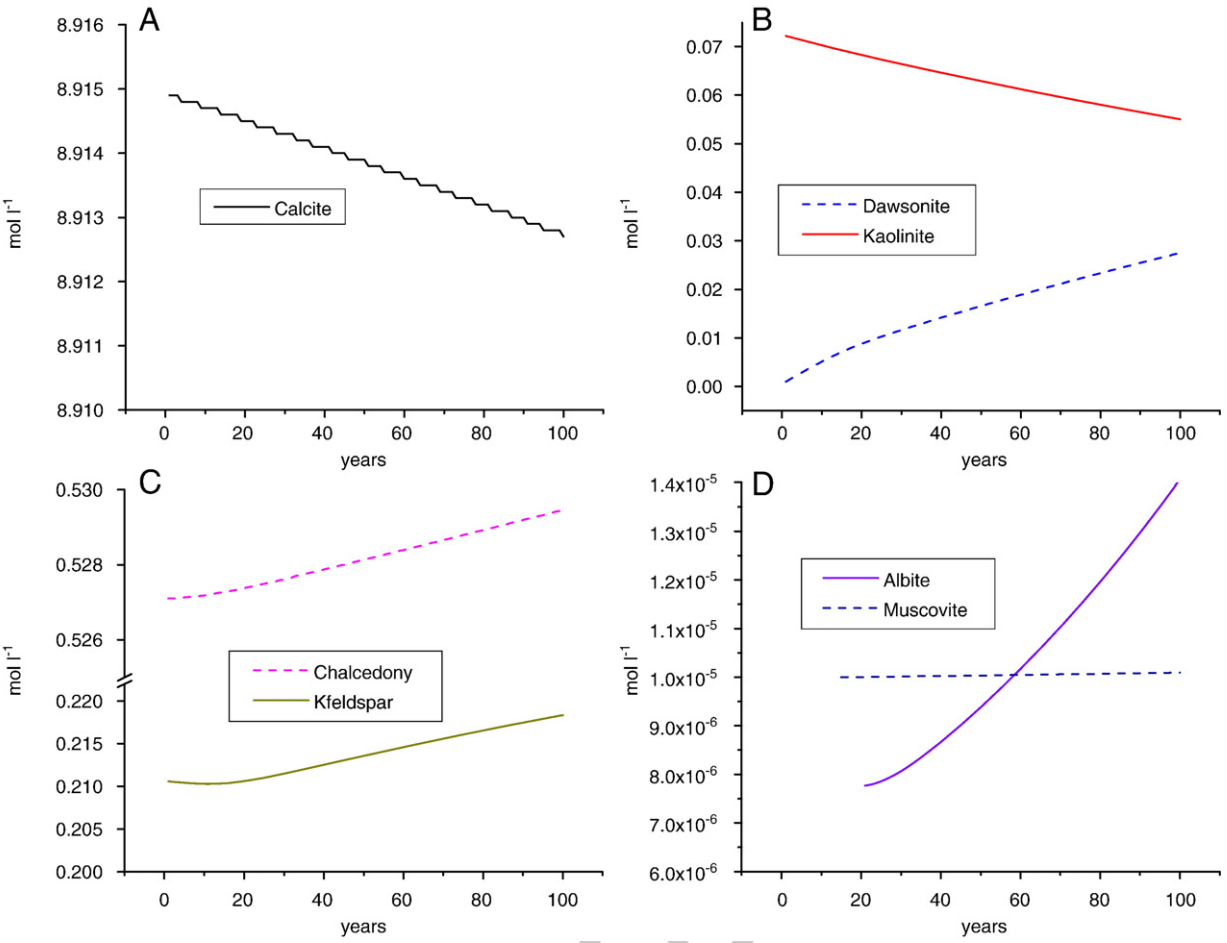

Fig. 6. Variation of solid species in Marly reservoir under CO_2–water–rock interaction for 100 years: A: calcite, B: dawsonite and kaolinite, C: chalcedony and K-feldspar, and D: albite and muscovite. Disordered dolomite and pyrite are not shown.

4.3 molal. The general form of these equations can be found in Duan et al. (1992). According to their model, under the WOF conditions (62 °C and 15 MPa) the fugacity of CO_2 is 7.32 MPa. Fugacity of CO_2 was set in PHREEQC as partial pressure. Kinetic simulations were performed for a time span of 100 years through 100 successive incremental steps. To each step, rates of kinetic reactions are integrated for incremental times t_i. The resulting system is equilibrated with CO_2; thus, the results of the previous time step are the starting point of the successive one.

Thermo-kinetic modeling of the temporal evolution for the WOF system shows a roughly decrease of pH from 6.91 to 5.07 and from 6.76 to 5.31 for the Marly and Vuggy reservoirs, respectively. The main variation is achieved after 1 year of simulation. After this period, in the Marly reservoir pH continues to decrease, whereas it maintains relatively constant value in the Vuggy reservoir. Temporal evolution of solid species in Marly and Vuggy reservoirs subjected to CO_2 injection are showed in Figs. 6 and 7.

High H^+ concentrations favor the calcite dissolution in both reservoirs (6.08×10^{-3} and 1.7×10^{-3} mol·l^{-1} for Marly and Vuggy, respectively). Although equilibrium is predicted to be achieved in less than 1 year, calcite continues to dissolve even after 100 years (see Section 6.3) up to 8.26×10^{-3} mol·l^{-1} in the Marly reservoir. The influence of disordered dolomite (not shown in Figs. 6 and 7) can be considered negligible in both reservoirs, since it only dissolves 9.13×10^{-6} (Marly) and 3.31×10^{-6} mol·l^{-1} (Vuggy). Carbonate dissolution causes a strong increase of Ca^{2+} and HCO_3^- concentrations during the first year of simulation (up to 2.524×10^{-3} and 1.44×10^{-1} mol·l^{-1}, respectively). Among carbonate minerals, dawsonite starts to precipitate even during the first year (4.981×10^{-4} and 3.49×10^{-5} mol·l^{-1} in the Marly and Vuggy reservoirs, respectively), achieving concentrations of 2.73×10^{-2} (Marly) and 1.74×10^{-3} (Vuggy) mol·l^{-1} after 100 years. Chalcedony precipitates in both reservoirs (2.33×10^{-3} and 3.19×10^{-4} mol·l^{-1} in the Marly and Vuggy aquifers, respectively). Al-silicates show a different behavior in the Marly and Vuggy reservoirs. In the former, the CO_2 injection induces dissolution of kaolinite (from 7.26×10^{-2} to 5.5×10^{-2} mol·l^{-1} after 100 years), whereas K-feldspar, after an initial dissolution (about 4×10^{-4} mol·l^{-1}) within the first 14 years of simulation, precipitates with muscovite and albite with concentrations of 0.218, 1.009×10^{-5} and 1.40×10^{-5} mol·l^{-1}, respectively. In the Vuggy reservoir, kaolinite dissolves more slowly than in the Marly aquifer. This implies that K-feldspar is still dissolving even when muscovite starts precipitating as secondary mineral. Concentrations of Si, chalcedony controlled, constantly increase in both reservoirs (about 6.82×10^{-3} mol·l^{-1}) due to CO_2 weathering (e.g., Golubev et al., 2005; Navarre-Sitchler and Brantley, 2007). After 100 years no Al-silicates are able to achieve equilibrium condition. Potassium derived from the dissolution/precipitation of K-feldspar is partially fixed in the reservoir as muscovite. Pyrite (not shown in Figs. 6 and 7) seems to play a negligible role. Anhydrite and gypsum are not formed after 100 years.

6. Discussion

6.1. Critical aspect of the reconstruction of the in-situ reservoir composition (62 °C, 15 MPa)

The pre-injection chemical composition of the Marly and Vuggy water reservoirs was calculated by assuming thermodynamic equilibrium among solid, aqueous and gas phases. As previously mentioned, geochemical interactions with the oil phase, the dissolved organic species and the water-flooding processes were neglected in the

Please cite this article as: Cantucci, B., et al., Geochemical modeling of CO_2 storage in deep reservoirs: The Weyburn Project (Canada) case study, Chemical Geology (2009), doi:10.1016/j.chemgeo.2008.12.029

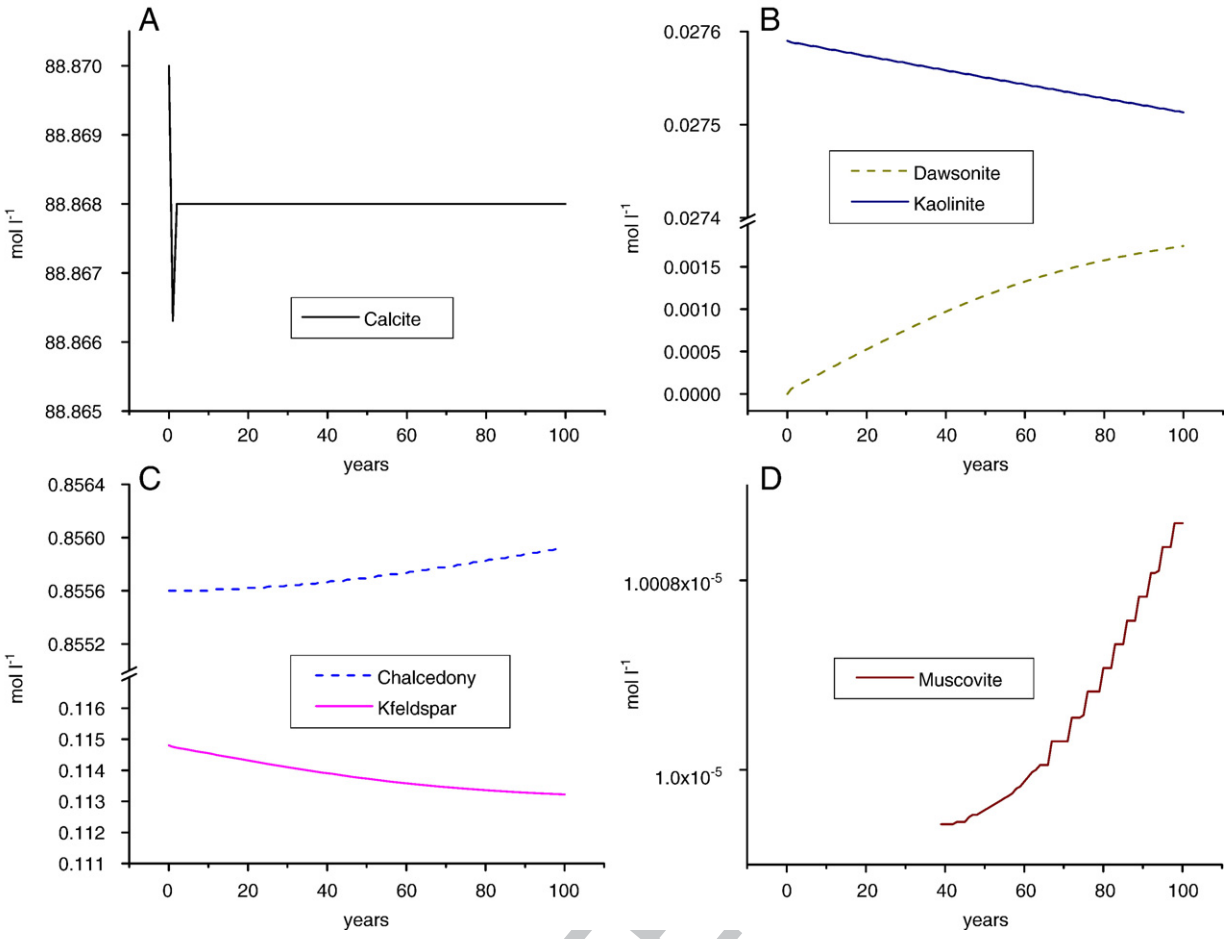

Fig. 7. Variation of solid species in Vuggy reservoir under CO_2–water–rock interaction for 100 years. A: calcite, B: dawsonite and kaolinite, C: chalcedony and K-feldspar, D: muscovite. Disordered dolomite and pyrite are not shown.

simulations because no data were available. These simplifications are critical for the numerical simulations because gas partitioning in the oil phase and the presence of organic compounds in solution may seriously affect the obtained results. On the other hand, water-flooding could invalidate the initial hypothesis of thermodynamic equilibrium among present phases in the WOF. The validation procedure (see below) is an important tool to verify the extent of such approximation.

From the surface to the reservoir water chemical composition significantly changes, e.g., Ca^{2+} and Mg^{2+} concentrations decrease from 1 to 4 orders of magnitude due to calcite and disordered dolomite precipitation. Several authors (e.g., Willey et al., 1975; Merino, 1979) suggest that calcite and dolomite over-saturation may result from a) CO_2 degassing during fluid uprising favoring carbonate precipitation and b) erroneous alkalinity data since no reliable information on organic acid anions are available.

Equilibrium simulation for waters collected at surface and a multi-component CH_4-rich gas phase allow redox reactions reproducing reduction process from SO_4^{2-} to HS^-, typical of many oil reservoirs (e.g., Aharon and Fu, 2000). Methane reacts with the sulfates (i.e., anhydrite and gypsum) to form calcite and H_2S, as described by the following reaction (Feely and Kulp, 1957):

$$CH_4 + CaSO_4 \leftrightarrow CaCO_3 + H_2S + H_2O. \quad (6)$$

This reaction causes a sharp decrease in the concentration of SO_4^{2-} and consequently, aqueous HS^- increases, favoring the dissolution of anhydrite and gypsum.

Sulfate reduction can be either thermo-chemical or mediated by bacteria (e.g., Gavrieli et al., 1995; Marini et al., 2000). The latter also provokes an increase of HS^- and carbonate precipitation through a reaction analogous to reaction (6). As the concentration of sulfide increases, pyrite precipitates, leading to a decrease in the concentration of Fe.

From surface to reservoir K-feldspar partially dissolves, whereas chalcedony and kaolinite precipitate; consequently K^+ and Al concentrations are expected to increase. Furthermore, the presence of organic ligands enhances the cation contents in the water phase (Wang et al., 1983; Bénézeth et al., 1994). Nevertheless, the lack of analytical data related to the abundances of organic acids in the Weyburn brine may have led to an underestimation of Ca, Mg, Fe, Al content (Giordano and Kharaka, 1994) when an inorganic model is applied.

Finally, the concentrations of conservative species, such as Na^+, Cl^- and Li do not show significant variations.

6.2. Critical aspects of reconstruction of the "initial" brine composition (62 °C, 15 MPa)

The "initial" brine composition of the Marly and Vuggy reservoirs was calculated by assuming thermodynamic equilibrium among the WOF mineralogical assemblage, the NaCl equivalent brine (with a Cl/Na ratio similar to that of seawater, i.e., 1.2) and the multi-component free gas-cap composition. Also in these simulations, geochemical interactions with the oil phase, the dissolved organic species and the water-flooding were not considered.

For most analytical species and pH values, the chemical composition of the "initial" brine results to be similar to that of the selected wells for each reservoir calculated at the same reservoir conditions. This is due to the fact that the composition of the formation waters is mainly controlled

Please cite this article as: Cantucci, B., et al., Geochemical modeling of CO_2 storage in deep reservoirs: The Weyburn Project (Canada) case study, Chemical Geology (2009), doi:10.1016/j.chemgeo.2008.12.029

by equilibrium with mineral and gas phases (e.g., Bazin et al., 1997; Palandri and Reed, 2001). Nevertheless, the concentrations of some species (K^+, HCO_3^-, Ca^{2+}, Mg^{2+}, SO_4^{2-} in the Marly and K^+, Cl^-, Al, in the Vuggy) show significant differences (Table 6). These variations can be due to various causes that strongly modify the WOF original chemical composition, such as a) natural variability in the salinity (and chemical composition) of the WOF waters (TDS 23–107 g·l^{-1}), b) water-flooding processes for more than 36 years for each sector of WOF; c) oil chemical interaction with other phases and d) microbial activity, specially related to the oil phase. Furthermore, a possible overestimation of Al should also be taken into account.

6.3. Critical aspect in the geochemical impact of CO_2 injection after 100 years

The reconstruction of the WOF "initial" brine composition can allow to *i)* evaluate the geochemical impact of the CO_2 injection up to 100 years and *ii)* quantify the geochemical capacity of CO_2 storage (solubility and mineral trapping) of the Weyburn reservoir after this period. Geochemical impact of supercritical CO_2 was simulated assuming a saturation condition between aqueous and pure CO_2 gas phase.

Dissolution of CO_2 in the Marly and Vuggy aquifers produces a sharp decrease of the pH values after a few years of simulation, inducing chemical reactions able to re-establish equilibrium conditions (Figs. 6 and 7). From a kinetic point of view the fast-reacting solid phases are carbonate minerals (e.g., calcite). In the Marly and Vuggy reservoirs calcite quickly dissolves within the first year, whereas reactions involving disordered dolomite can be considered negligible. In the Vuggy reservoir pH values steadily increase up to 5.31 within the first year, whereas in the Marly aquifer it continues to decrease for 100 years (down to 5.07). This different behavior is likely due to reactions involving Al-silicate minerals. In the very first years of simulation, CO_2 injection into the Marly reservoir produces a partial dissolution of K-feldspar and kaolinite, with the formation of muscovite and albite after 16 and 22 years, respectively. Precipitation of secondary minerals and K-feldspar releases H_2CO_3 in solution with consequent pH decrease. In the Vuggy reservoir, alteration of K-feldspar and kaolinite leads, after 37 years, to muscovite precipitation, likely due to minor amount of Na^+ in solution. After 100 years, Al-silicates do not achieve equilibrium conditions. Kinetic simulations suggest that dissolution of carbonate and Al-silicate minerals, catalyzed by high concentrations of Na^+, favors the precipitation of dawsonite in both the WOF reservoirs (Johnson et al., 2001):

$$\underset{(K\text{–feldspar})}{KAlSi_3O_8} + Na^+ + CO_{2(aq)} + H_2O \leftrightarrow \underset{(\text{dawsonite})}{NaAlCO_3(OH)_2} + 3SiO_2 + K^+$$

Dawsonite precipitation in reservoirs subjected to CO_2 injection has been the object of several studies in the last few years. Most numerical models indicate that, under certain conditions (e.g., CO_2 fugacity higher than 2 MPa; Moore et al., 2005; Zerai et al., 2006), this mineral plays an important role in the CO_2 mineral trapping. More recently, Bénézeth et al. (2007) re-evaluated the thermodynamic proprieties of this mineral and the factors that control its formation. These authors estimated the relative stability of dawsonite with respect to Al- (bayerite or boehmite) and Na-bearing phases (albite) in geological environment typical of CO_2 geological storage (100 °C, and total sodium concentration of 1.0 mol·kg^{-1}). They showed that the CO_2-induced dissolution of silica-bearing rocks (i.e., albite) in contact with saline solution buffers pH and imposes tight constraints on the formation of dawsonite. To ascertain the presence of dawsonite in the WOF system, the thermodynamic data of Bénézeth et al. (2007) were applied to our aqueous speciation model to calculate the Saturation Index of dawsonite. The computed Saturation Index (1.18 and 1.52, in Marly and Vuggy respectively) indicates that after 1 year from CO_2 injection the precipitation of dawsonite can occur. In the Marly reservoir dawsonite mainly precipitates due to the dissolution of kaolinite. In our model kaolinite was set as proxy for clay mineral. Thus, this approximation can be regarded as a conservative one, this mineral playing a key role as both Al source and dawsonite precipitation.

Dawsonite precipitates after 1 year of simulation reaching, after 100 years, relatively high concentrations (2.75×10^{-2} and 1.74×10^{-3} mol·l^{-1} in the Marly and in the Vuggy reservoirs, respectively). Dawsonite precipitation associated with the release of Si from the alteration of Al-silicates leads to significant chalcedony formation. Pyrite remains unchanged and no anhydrite (in the Vuggy) or gypsum (in the Marly) is formed after 100 years.

6.4. Geochemical trapping mechanisms

The CO_2 injected into a geological reservoir can be trapped through two main geochemical processes (Gunter et al., 1993): *i) solubility trapping*, where the acidic gas is dissolved in solution as $CO_{2(aq)}$, ions and carbonate complexes (e.g., HCO_3^-, $CaHCO_3^+$, etc.) and *ii) mineral trapping*, with formation of secondary stable carbonate minerals.

Kinetic modeling of the temporal evolution of the Weyburn reservoirs subjected to CO_2 injection over 100 years shows that "solubility trapping" is the prevailing process in the early stages, being the amount of dissolved CO_2 equals to 0.76 and 0.87 mol·l^{-1} for the Marly and Vuggy aquifers, respectively (Fig. 8). A smaller volume of injected CO_2 is likely trapped as ions (i.e., HCO_3^-, 0.14 mol·l^{-1}) and carbonate complexes (e.g., $NaHCO_{3(aq)}$, $CaHCO_{3(aq)}^+$; 0.1394 and 0.18 mol·l^{-1} for the Marly and Vuggy reservoirs). Over 100 years, a significant quantity of the injected CO_2 is trapped as dawsonite (0.027 and 0.002 mol·l^{-1} for the Marly and Vuggy reservoirs, respectively). The mass balance, calculated as the difference between dissolved (calcite and dolomite) and precipitated (dawsonite) carbonate minerals (Fig. 8), shows that 0.019 (Marly reservoir) and 5.69×10^{-5} (Vuggy reservoir) mol·l^{-1} of CO_2 are effectively trapped. After this period dawsonite is still precipitating, whereas calcite and dolomite are in equilibrium. It is highly likely that mineral trapping may increase, once the simulation is carried out over a longer period (10 000–250 000 years).

7. Validation of geochemical model (path D–E)

Owing to the chemical complexity of water–CO_2–rock interaction processes in deep reservoirs, geochemical modeling requires assumptions, uncertainties and approximation. Moreover, the reliability of geochemical modeling can also be jeopardized by the scarcity of information on the reservoir and the unavailability of kinetic reaction rates, e.g., precipitation rates. Hence, the numerical simulations, able to describe the physico-chemical processes of CO_2 storage at WOF, have been validated by comparing the computed data with the analytical results obtained at the wellhead in September 2003 (Table 1). Numerical validation of our simulations was performed by means of PHREEQC

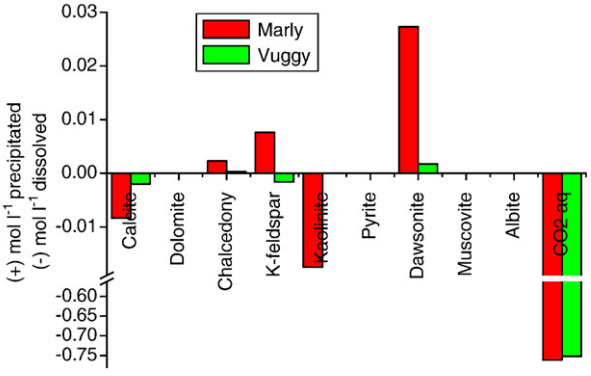

Fig. 8. Comparison of the mineralogical changes at reservoir conditions (62 °C, 15 MPa) between Marly (red) and Vuggy (green) reservoirs due to CO_2 injection after 100 years. (For interpretation of the references to colour in this figure legend, the reader is referred to the web version of this article.)

Please cite this article as: Cantucci, B., et al., Geochemical modeling of CO_2 storage in deep reservoirs: The Weyburn Project (Canada) case study, Chemical Geology (2009), doi:10.1016/j.chemgeo.2008.12.029

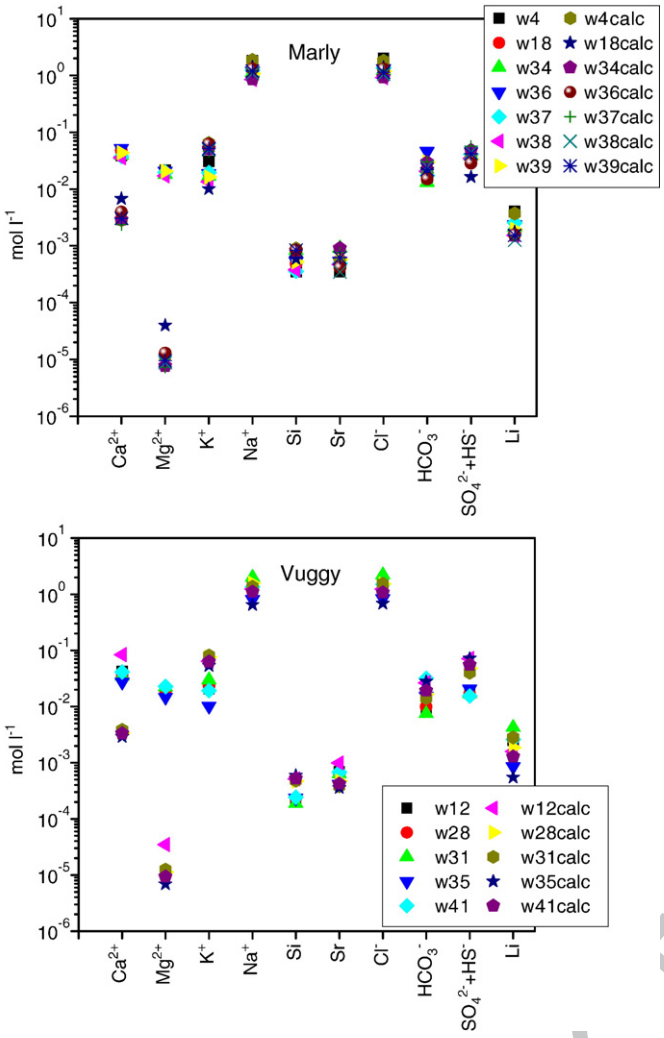

Fig. 9. Comparison between the 2003 calculated and analytical chemical composition of selected waters of Marly (above) and Vuggy (under) reservoirs.

code. Starting from the pre-injection reservoir chemical and mineralogical composition (Table 6), the supercritical CO_2 injection into the WOF for 3 years (from 2000 to 2003) was simulated (Fig. 3, path D). Fluid–rock–CO_2 interactions were performed through kinetically-controlled reactions, by using Eqs. (3) and (4) and thermodynamic parameters presented in Table 2. Kinetic simulation for each reservoir was carried out for isothermal conditions of 62 °C, constant pressure of 15 MPa and pure CO_2 fugacity of 7.32 MPa. Dissolution kinetic rate for supercritical CO_2 in solution is not defined, although it can reasonably be assumed fast when compared with that of the Al-silicates considered in this study. In order to simulate the CO_2 injection, a specific amount of $CO_{2(g)}$, corresponding to the estimated CO_2 volume injected in the Marly and Vuggy reservoirs in 2000–2003 time span (70.75×10^9 mol of CO_2 in May 2003; Tian et al., 2004), was considered. Assuming a constant injection rate with time, in September 2003 about 79.33×10^9 mol of CO_2 were injected into the two aquifers. As the injection rate for each reservoir is unknown, the whole volume of injected CO_2 has been assumed to be reacting. By considering the porosity and the average rock volume of the Marly (26% and 2.66×10^8 m^3, respectively) and Vuggy (14% and 1.87×10^8 m^3, respectively) reservoirs, the molar concentration of CO_2 injected in 3 years was calculated to be 0.33 and 0.47 mol·l^{-1}, respectively.

In order to compare the results obtained by the kinetic simulation with the analytical data, the outgassing of the reservoir waters towards the surface (temperature, pressure and boundary conditions) was performed (path E) by: i) decreasing the temperature of CO_2-rich reservoir waters from 62 to 25 °C and ii) equilibrating the aqueous solutions at the surface pressure (0.1 MPa) with air (78% N_2, 20.9% O_2, 0.00005% H_2 and 0.03% CO_2) without considering any interaction between the host-rock minerals and the fluids. As it is not possible to quantify the mineral precipitation due to the fluid degassing, the geochemical interactions between minerals and fluids have not been considered. The calculated concentrations of SO_4^{2-} and HS^- have been summed up and compared with those of the measured sulfates (Table 1).

The comparison between computed and analytical concentrations after 3 years was carried out by both a numerical and a statistical approach. The numerical comparison between simulated and analytical results (Fig. 9) shows a good correspondence for most analytical species (i.e., HCO_3^-, Cl^-, Na^+, Li, SO_4^{2-}+HS^-, Sr and Si; Fig. 9), although the measured contents of Ca^{2+} and Mg^{2+} are 1 to 3 orders of magnitude higher than those calculated (Table 7).

The calculated concentrations of the main species with respect to the analytical data show the same variations for the period 2000–2003. Conservative species, such as Cl^-, Na^+, and Li slightly increases (from 1.20, 1.19, 1.69×10^{-3} mol·l^{-1} for the baseline to 1.34, 1.23 and 2.37×10^{-3} mol·l^{-1} for September 2003, respectively) in both simulated and analytical data. Concentrations of SO_4^{2-}+HS^- display an increase from 2000 (3.59×10^{-2} mol·l^{-1}) to 2003 (3.68 and 4.67×10^{-2} mol·l^{-1} for the analytical and calculated concentrations, respectively) for both simulated and analytical data.

Strontium concentrations behave differently since the analytical data tend to decrease from 2000 (5.46×10^{-4} mol·l^{-1}) to 2003 (4.30×10^{-4} mol·l^{-1}), where those calculated increase from the baseline to September 2003 (5.74×10^{-4} mol·l^{-1}).

Analytical and calculated concentrations of Si increase in both simulated and analytical data (from 4.240×10^{-4} mol·l^{-1} for the baseline to 5.36×10^{-4} mol·l^{-1} in 2003).

In both reservoirs the calculated K^+ concentrations are about 40% higher than those measured. This may be due to an overestimation of the K-feldspar dissolution rate and/or the reactive surface area. Reaction rates for feldspars are very uncertain as suggested by the

Table 7
Calculated chemical composition (mol·l^{-1}) of selected waters of WOF after 3 years of CO_2 injection at surficial conditions of 25 °C and 0.1 MPa

Reservoir	Well	Location	pH	Na^+	K^+	Ca^{2+}	Mg^{2+}	HCO_3^-	Cl^-	SO_4^{2-}+HS^-	Li	Sr	Si
Marly	w 04	14-1 6-14	6.00	1.87	6.40×10^{-2}	2.84×10^{-3}	1.16×10^{-5}	1.87×10^{-2}	1.80	3.76×10^{-2}	3.70×10^{-3}	5.35×10^{-4}	8.95×10^{-4}
	w 18	b 8-18 6-13	6.17	1.39	1.00×10^{-2}	6.78×10^{-3}	3.96×10^{-4}	2.18×10^{-2}	1.38	1.63×10^{-2}	1.75×10^{-3}	4.35×10^{-4}	5.91×10^{-4}
	w 34	d 14-18 6-13	6.26	0.86	5.07×10^{-2}	2.89×10^{-3}	7.71×10^{-6}	2.96×10^{-2}	0.93	4.83×10^{-2}	1.53×10^{-3}	9.10×10^{-4}	8.25×10^{-4}
	w 36	d14-11 6-14	5.96	1.30	6.21×10^{-2}	3.96×10^{-3}	1.29×10^{-5}	1.49×10^{-2}	1.30	2.86×10^{-2}	1.58×10^{-3}	4.17×10^{-4}	8.43×10^{-4}
	w 37	2-10 6-14	6.26	1.15	4.61×10^{-2}	2.36×10^{-3}	7.30×10^{-6}	3.01×10^{-2}	1.27	5.69×10^{-2}	1.53×10^{-3}	7.58×10^{-4}	8.40×10^{-4}
	w 38	14-14 6-14	6.18	1.08	4.91×10^{-2}	3.04×10^{-3}	8.70×10^{-6}	2.49×10^{-2}	1.04	4.42×10^{-2}	1.26×10^{-3}	3.46×10^{-4}	8.42×10^{-4}
	w 39	b14-13 6-14	6.13	1.19	5.16×10^{-2}	3.04×10^{-3}	9.53×10^{-6}	2.21×10^{-2}	1.13	4.16×10^{-2}	1.53×10^{-3}	6.16×10^{-4}	8.39×10^{-4}
Vuggy	w 12	d 8-7 6-13	6.19	1.24	6.43×10^{-2}	8.40×10^{-3}	3.50×10^{-5}	2.64×10^{-2}	1.24	7.14×10^{-2}	1.58×10^{-3}	9.95×10^{-4}	5.14×10^{-4}
	w 28	10-17 6-13	5.98	1.57	7.63×10^{-2}	3.35×10^{-3}	1.13×10^{-5}	1.65×10^{-2}	1.53	4.83×10^{-2}	1.86×10^{-3}	4.73×10^{-4}	4.69×10^{-4}
	w 31	d 14-6 6-13	5.91	1.36	8.07×10^{-2}	3.83×10^{-3}	1.25×10^{-5}	1.41×10^{-2}	1.54	4.02×10^{-2}	2.83×10^{-3}	3.81×10^{-4}	4.81×10^{-4}
	w 35	12-25 -14	6.22	0.65	5.32×10^{-2}	2.90×10^{-3}	6.89×10^{-6}	2.79×10^{-2}	0.68	7.20×10^{-2}	5.46×10^{-3}	3.59×10^{-4}	5.94×10^{-4}
	w 41	d 8-23 6-14	5.97	1.10	6.31×10^{-2}	3.33×10^{-3}	9.40×10^{-6}	1.93×10^{-2}	1.07	5.53×10^{-2}	1.29×10^{-3}	4.24×10^{-4}	5.23×10^{-4}

t8.1 **Table 8**
Results of median test applied to our geochemical model for the Marly and Vuggy reservoirs, with significant level of $\alpha<0.05$

t8.3 α	pH	HCO_3^-	Ca^{2+}	Cl^-	K^+	Li	Mg^{2+}	Na^+	Si	Sr	$SO_4^{2-}+HS^-$
t8.4 0.05											
t8.5 Marly	0.567	0.567	**0.001**	1.000	**0.001**	0.080	**0.001**	1.000	**0.015**	1.000	0.567
t8.6 Vuggy	**0.029**	0.486	**0.029**	0.486	**0.029**	0.486	**0.029**	0.486	1.000	0.486	**0.029**

t8.7 Results for which the difference of medians between group 1 and 2 is statistically significant are in bold.

large variability (100–1000 times) of results obtained during different experimental runs (e.g., Busenberg and Clemency, 1976; Lagache, 1976; Helgeson et al., 1984; Manley and Evans, 1986; Holdren and Speyer, 1987; Bevan and Savage, 1989; Rafal'skiy et al., 1990; Sverdrup, 1990; Gautier et al., 1994; Blum and Stillings, 1995; Blake and Walter, 1996; Alekseyev et al., 1997; Blake and Walter, 1999; Teng et al., 2001; Fenter et al., 2003).

According to the calculated and analytical data, three years of CO_2 injection in the WOF induces a decrease of the pH values (6.51–6.75 for the baseline and 6.33–6.39 in September 2003), although the analytical pH values are affected by degassing. The CO_2 injection enhances the dissolution of carbonate minerals, mainly calcite. This leads to an increase of the analytical concentrations of HCO_3^- (up to 7 times in 2003) with respect to that of the baseline. The gas loss during sampling can be a key factor to explain this difference. Calcium and magnesium concentrations increase after the injection of CO_2. Nevertheless the measured Ca^{2+} and Mg^{2+} contents are 10 to 1000 times higher than the calculated ones (Table 7), likely due to the presence of carboxylic acid acting as complexant agent (Kharaka et al., 2006). Organic species (not available for present study) in formation waters play an important role in mineral diagenesis (Surdam et al., 1989; Seewald, 2001) as they act as proton donors for a variety of pH-dependent reactions and can contribute to the water alkalinity (Lundegard and Land, 1986).

In order to evaluate from a statistical point of view our geochemical model, the computed and measured analytical data of September 2003 have been compared by using the non-parametric Median Test. For each reservoir and for each considered variable (i.e., pH, HCO_3^-, Ca^{2+}, Cl^-, K^+, Li, Mg^{2+}, Na^+, Si, Sr, $SO_4^{2-}+HS^-$) two groups can be defined: a) the modeled surficial data and b) the analytical data of waters at September 2003. Then, the null hypothesis H_0, i.e., the data for each variable have been extracted from populations with the same medians (when its probability is higher than 0.05), was formulated.

The results of Median Test show (Table 8) that the null hypothesis can be accepted for HCO_3, Cl^-, Na^+, Li, Sr, for Marly and Vuggy reservoirs, Si for the Vuggy and pH and $SO_4^{2-}+HS^-$ for the Marly, with the exception of Ca^{2+}, Mg^{2+}, and K^+. The two earth alkaline elements are likely affected by the presence of carboxylic acid, whereas the calculated K^+ contents reflect the overestimation of the K-feldspar kinetic reaction rate.

8. Conclusions

Geochemical modeling applied to deep CO_2 storage reservoirs (>800 m) is an important tool to define equilibrium conditions among the various phases and to investigate the short- to long-term consequences of CO_2 injection. The *International Energy Agency (IEA) Weyburn CO_2 Monitoring & Storage Project* was chosen as "case study" to test a new geochemical approach that includes five main paths (Fig. 3): A) calculation of the reservoir chemical composition (62 °C and 15 MPa) for the Marly and Vuggy waters on the basis of surface pre-injection analytical data; B) identification of the composition of the original Marly and Vuggy fluids ("initial" brines); C) evaluation of the geochemical impact of CO_2 injection in the Weyburn Oil Field (WOF) system for 100 years via kinetically-controlled reactions; D–E) validation of geochemical modeling comparing the analytical (collected in September 2003) and the simulated data. First the simulation of the CO_2 injection in the WOF for 3 years via kinetically-controlled reactions was computed. Successively, the "reservoir to surface" uprising processes to which the deep-seated fluids are subjected were reconstructed.

The a posteriori procedure, involving the analytical data of samples collected at wellhead, were used to: *i)* reconstruct the in-situ reservoir chemical composition, *ii)* identify chemical composition of the initial aqueous liquid phases at pre-injection conditions for both reservoirs, and *iii)* simulate the system evolution after 3 (see Section 7) and 100 years. The simulations presented in this paper are constrained by some assumptions of the physico-chemical processes expected to occur in a complex system subjected to CO_2 storage such as the WOF. The main approximation is that to have neglected the interaction with oil phase. Thus the calculated pH, saturation indexes and speciation may be different if the oil phase is taken into account. Other uncertainties are related to the unavailability of thermodynamic and kinetic data (Xu et al., 2004, 2007; Gherardi et al., 2007; Marini, 2007). Despite these assumptions and simplifications, the statistical Median Test, used to compare computed and measured data, suggests that the proposed geochemical model is able to reliably describe the real behavior of most investigated variables with the exception of Ca^{2+}, Mg^{2+} and K^+, likely due to complexation effects induced by the organic fraction (Kharaka et al., 2006) and overestimation of the K-feldspar kinetic reaction rate, respectively.

The geochemical simulations allow to suggest that injected CO_2 at the Weyburn Oil Field is partially neutralized by solubility (as $CO_{2(aq)}$) and mineral trapping (through dawsonite precipitation). New software implementation coupled with a detailed sampling and analyzing deep fluids, both in pre- and post-CO_2 injection phases, may result in a specific monitoring protocol for the Regulation and Policy CCS Community, particularly if not conventional monitoring technologies, such as U-tube system, are used.

9. Uncited references

Q5

Rafal'skiy and Prisyagina, 1991
Wagman et al., 1976

Acknowledgments

The authors wish to express their gratitude to Pascale Bénézeth, Yousif K. Kharaka and Renee J. Perez whose comments have improved an early version of the manuscript. Many thanks are due to Antonella Buccianti for her helpful and useful suggestions related to the statistical part. Daniele Cinti is warmly thanked for his assistance during the chemical analysis of the WOF waters. Discussions with Luca Pizzino, Nunzia Voltattorni and Alessandra Sciarra have been appreciated. This work was realized in the framework of a collaboration between the International Energy Agency Weyburn CO_2 Monitoring & Storage Project (Project Director, Ray Knudsen) and INGV.

References

Aharon, P., Fu, B., 2000. Microbial sulfate reduction rates and sulfur and oxygen isotope fractionations at oil and gas seeps in deepwater Gulf of Mexico. Geochimica et Cosmochimica Acta 64, 233–246.

Alekseyev, V.A., Medvedeva, L.S., Prisyagina, N.I., Meshalkin, S.S., Balabin, A.I., 1997. Change in the dissolution rates of alkali feldspars as a result of secondary mineral precipitation and approach to equilibrium. Geochimica et Cosmochimica Acta 61, 1125–1142.

Please cite this article as: Cantucci, B., et al., Geochemical modeling of CO_2 storage in deep reservoirs: The Weyburn Project (Canada) case study, Chemical Geology (2009), doi:10.1016/j.chemgeo.2008.12.029

Arnórsson, S., 1999. Progressive water–rock interaction and mineral solution equilibria in groundwater systems. In: Ármannsson, H. (Ed.), Geochemistry of the Earth's Surface. Balkema, Rotterdam, pp. 471–474.

Arnórsson, S., Andrésdóttir, A., 1995. Processes Controlling the Chemical Composition of Natural Waters in the Hreppar–Land Area in Southern Iceland, vol. 788. International Atomic Energy Agency, pp. 21–43. IAEA TECDOC.

Arnórsson, S., Gunnlaugsson, E., Svavarsson, H., 1983. The chemistry of geothermal waters in Iceland. II. Mineral equilibria and independent variables controlling water compositions. Geochimica et Cosmochimica Acta 47, 547–566.

Bailey, N.J.L., Krouse, H.R., Evans, C.R., Rogers, M.A., 1973. Alteration of crude oil by waters and bacteria. Evidence from geochemical and isotope studies. AAPG Bulletin 57, 1276–1290.

Ball, J.W., Nordstrom, D.K., 1991. User's Manual for WATEQ4F, with revised thermodynamic data base and test cases for calculating speciation of major, trace, and redox elements in natural waters. United States Geological Survey Open-File Report 91-183. United States Geological Survey, Menlo Park, California.

Bazin, B., Brosse, E., Sommer, F., 1997. Reconstitution de la chimie des eaux de gisement en réservoir gréseux en vue d'une modélisation numérique de la diagènese minérale. Bulletin de la Société Géologique de France 168, 231–242.

Bénézeth, P., Castet, S., Dandurand, J.-L., Gout, R., Schott, J., 1994. Experimental study of aluminum-acetate complexing between 60 and 200 °C. Geochimica et Cosmochimica Acta 58 (21), 4561–4571.

Bénézeth, P., Palmer, D.A., Wesolowski, D.J., 2001. Aqueous high-temperature solubility studies. II. The solubility of boehmite at 0.03 m ionic strength as a function of temperature and pH as determined by in situ measurements. Geochimica et Cosmochimica Acta 65 (13), 2097–2111.

Bénézeth, P., Palmer, D.A., Anovitz, L.M., Horita, J., 2007. Dawsonite synthesis and reevaluation of its thermodynamic properties from solubility measurements: implications for mineral trapping of CO_2. Geochimica et Cosmochimica Acta 71, 4438–4455.

Berner, R.A., Holdren, G.R., 1979. Mechanism of feldspar weathering. II: observations of feldspars from soils. Geochimica et Cosmochimica Acta 43, 1173–1186.

Berner, R.A., Schott, J., 1982. Mechanism of pyroxene and amphibole weathering II. Observations of soil grains. American Journal of Science 282, 1214–1231.

Bevan, J., Savage, D., 1989. The effect of organic acids on the dissolution of K-feldspar under conditions relevant to burial diagenesis. Mineralogical Magazine 53, 415–425.

Blake, R.E., Walter, L.M., 1996. Effects of organic acids on the dissolution of orthoclase at 80 °C and pH 6. Chemical Geology 132, 91–102.

Blake, R.E., Walter, L.M., 1999. Kinetics of feldspar and quartz dissolution at 70–80 °C and near-neutral pH: Effect of organic acids and pH. Geochimica et Cosmochimica Acta 63, 2043–2059.

Blum, A.E., Stillings, L.L., 1995. Feldspar dissolution kinetics. In: White, A.F., Brantley, S.L. (Eds.), Chemical Weathering Rates of Silicate Minerals. Mineralogical Society of America, Washington, D.C., pp. 291–351.

Burrowes, O.G., 2001. Investigating CO_2 storage potential of carbonate rocks during tertiary recovery from a billion barrel oil field, Weyburn Saskatchewan: Part 2 – reservoir geology (IEA Weyburn CO2 Monitoring and Storage Project). Summary of Investigations 2001, vol. 1. Saskatchewan Geological Survey, pp. 64–71. Sask. Energy Mines, Misc. Rep. 2001-4.1.

Busenberg, E., Clemency, C.V., 1976. The dissolution kinetics of feldspars at 25 °C and 1 atm CO_2 partial pressure. Geochimica et Cosmochimica Acta 40, 41–49.

Churcher, P.L., Edmunds, A.C., 1994. Reservoir characterization and geological study of the Weyburn Unit, Southeastern Saskatchewan. Report Number 1. Proposed miscible flood, horizontal well and waterflood optimization areas. PanCanadian Internal Commercial-in-Confidence Report, p. 85.

Codata Task Group, 1976. Codata recommended key values for thermodynamics. Journal of Chemical Thermodynamics 8, 603–605.

Ride, D.R. (Ed.), 2001. CRC handbook of chemistry and physic, 81 edition. CRC Press Llc, p. 2556.

Damen, K., Faaij, A., Turkenburg, W., 2006. Health, safety and environmental risks of underground CO_2 storage – overview of mechanisms and current knowledge. Climatic Change 74 (1–3), 289–318.

Duan, Z., Sun, R., 2003. An improved model calculating CO_2 solubility in pure water and aqueous NaCl solutions from 273 to 533 K and from 0 to 2000 bar. Chemical Geology 193, 257–271.

Duan, Z., Moller, N., Weare, J.H., 1992. An equation of state for the CH_4–CO_2–H_2O system: 1. Pure systems from 0 to 1000 °C and 0 to 8000 bar. Geochimica et Cosmochimica Acta 56, 2605–2617.

Duan, Z., Sun, R., Zhu, C., Chou, I.-M., 2006. An improved model for the calculation of CO_2 solubility in aqueous solutions containing Na^+, K^+, Ca^{2+}, Mg^{2+}, Cl^-, and SO_4^{2-}. Climatic Change 98, 131–139.

El Sayed, S.A., Baker, R., Churcher, P.L., Emunds, A.C., 1993. Multidisciplinary Reservoir Characterization and Simulation of the Weyburn Unit, vol. 45, 10. Society of Petroleum Engineers, pp. 930–934.

Emberley, S., Hutcheon, I., Shevalier, M., Durocher, K., Gunter, W.D., Perkins, E.H., 2004. Geochemical monitoring of fluid–rock interaction and CO_2 storage at the Weyburn CO_2-injection enhanced oil recovery site, Saskatchewan, Canada. Energy 29, 1393–1401.

Emberley, S., Hutcheon, I., Shevalier, M., Durocher, K., Mayer, B., Gunter, W.D., Perkins, E.H., 2005. Monitoring of fluid–rock interaction and CO_2 storage through produced fluid sampling at the Weyburn CO_2-injection enhanced oil recovery site, Saskatchewan, Canada. Applied Geochemistry 20, 1131–1157.

Feely, H.W., Kulp, J.L., 1957. Origin of Gulf Coast salt-dome sulphur deposits. AAPG Bulletin 41 (8), 1802–1853.

Fenter, P., Park, C., Cheng, L., Zhang, Z., Krekeler, M.P.S., Sturchio, N.C., 2003. Orthoclase dissolution kinetics probed by in situ X-ray reflectivity: effects of temperature, pH, and crystal orientation. Geochimica et Cosmochimica Acta 67, 197–211.

Ferrante, M.J., Stuve, J.M., Richardson, D.W., 1976. Thermodynamic data for synthetic dawsonite. U.S. Bureau of Mines Report Investigation, vol. 8129, p. 13. Washington, D.C.

Freifeld, B.M., Trautz, R.C., 2006. Real-time quadrupole mass spectrometer analysis of gas in borehole fluid samples acquired using the U-tube sampling methodology. Geofluids 6, 217–224.

Freifeld, B.M., Trautz, R.C., Kharaka, Y.K., 2005. The U-tube: a novel system for acquiring borehole fluid samples from a deep geologic CO_2 sequestration experiment. Journal of Geophysical Research 110, B10203. doi:10.1029/2005JB003735.

Gauss, I., Azaroual, M., Czernichowski-Lauriol, I., 2005. Reactive transport modelling of the impact of CO_2 injection on the clayey cap rock at Sleipner (North Sea). Chemical Geology 217 (3–4), 319–337.

Gautier, J.M., Oelkers, E.H., Schott, J., 1994. Experimental studies of K-feldspar dissolution rates as a function of chemical affinity at 150 °C and pH 9. Geochimica et Cosmochimica Acta 58, 4549–4560.

Gautier, J.M., Oelkers, E.H., Schott, J., 2001. Are quartz dissolution rates proportional to B.E.T. surface areas? Geochimica et Cosmochimica Acta 65, 1059–1070.

Gavrieli, I., Starinsky, A., Spiro, B., Aizenshtat, Z., Nielsen, H., 1995. Mechanisms of sulfate removal from subsurface calcium chloride brines: Heletz–Kokhav oilfields, Israel. Geochimica et Cosmochimica Acta 59 (17), 3525–3533.

Gherardi, F., Xu, T., Pruess, K., 2007. Numerical modeling of self-limiting and self-enhancing caprock alteration induced by CO_2 storage in a depleted gas reservoir. Chemical Geology 244, 103–129.

Giggenbach, W.F., 1980. Geothermal gas equilibria. Geochimica et Cosmochimica Acta 44, 2021–2032.

Giggenbach, W.F., 1981. Geothermal mineral equilibria. Geochimica et Cosmochimica Acta 45, 393–410.

Giggenbach, W.F., 1988. Geothermal solute equilibria derivation of Na–K–Mg–Ca geoindicators. Geochimica et Cosmochimica Acta 52, 2749–2765.

Giordano, T.H., Kharaka, Y.K., 1994. Organic ligand distribution and speciation in sedimentary basin brines, diagenetic fluids and related ore solutions. Geological Society of London, Special Publication 78, 175–202.

Golubev, S.V., Pokrovsky, O.S., Schott, J., 2005. Experimental determination of the effect of dissolved CO_2 on the dissolution kinetics of Mg and Ca silicates at 25 °C. Chemical Geology 217, 227–238.

Grandstaff, D.E., 1978. Changes in surface area and morphology and the mechanism of forsterite dissolution. Geochimica et Cosmochimica Acta 42, 1899–1901.

Gunter, W.D., Perkins, E.H., McCann, T.J., 1993. Aquifer disposal of CO_2-rich gases: reaction design for added capacity. Energy Conversion and Management 34, 941–948.

Gunter, W.D., Wiwchar, B., Perkins, E.H., 1997. Aquifer disposal of CO_2-rich gases: extension of the time scale of experiment for CO_2-sequestering reactions by geochemical modeling. Mineralogy and Petrology 59, 121–140.

Gunter, W.D., Perkins, E.H., Hutcheon, I., 2000. Aquifer disposal of CO_2-rich gases: modeling of water–rock reactions for trapping of acid wastes. Applied Geochemistry 15, 1085–1095.

Gunter, W.D., Bachu, S., Benson, S.M., 2004. The role of hydrogeological and geochemical trapping in sedimentary basins for secure geological storage for carbon dioxide. In: Baines, S.J., Worden, R.H. (Eds.), Geological Storage of Carbon Dioxide. Geological Society Special Publication, vol. 233, pp. 129–145. London, UK.

Helgeson, H.C., Murhpy, W.M., Aagaard, P., 1984. Thermodynamic and kinetic constraints on reaction rates among minerals and aqueous solutions. II. Rate constants, effective surface area, and the hydrolysis of feldspar. Geochimica et Cosmochimica Acta 48, 2405–2432.

Hemingway, B.S., Robie, R.A., 1977. The entropy and Gibbs free energy of formation of the aluminum ion. Geochimica et Cosmochimica Acta 41, 1402–1404.

Holdren, G.W., Speyer, P.M., 1987. Reaction rate-surface area relationships during the early stages of weathering. II. Data on eight additional feldspars. Geochimica et Cosmochimica Acta 51, 2311–2318.

Holloway, S., 1996. The Underground Disposal of Carbon Dioxide. Final report of Joule 2 Project No. CT92-0031. British Geological Survey, Keyworth, Nottingham, United Kingdom, p. 355.

Hull, C., Reed, M.H., Fisher, K., 1987. Chemical geothermometry and numerical unmixing of diluted waters of the San Bernardino valley region of southern California. Geothermal Resources Council Transactions 11, 165–184.

IEA (International Energy Agency), 2004. Prospects for CO_2 Capture and Storage. IEA/OECD, Paris, France.

IEA (International Energy Agency), 2006. Energy Technology Perspectives: Scenarios and Strategies to 2050. IEA/OECD, Paris, France.

IPCC (Intergovernmental Panel on Climate Change), 2005. In: Metz, B., Davidson, O., de Coninck, H.C., Loos, M., Mayer, L.A. (Eds.), Special Report on Carbon Dioxide Capture and Storage. Cambridge University Press, 32 Avenue of the Americas, New York, NY 10013-2473, USA, p. 628.

IPCC (Intergovernmental Panel on Climate Change). Climate change 2007: The Physical Science Basis. Contribution of Working Group I to the Fourth Assessment Report of the Intergovernmental Panel on Climate Change. Solomon, S.D., Qin, M., Manning, Z., Chen, M., Marquis, K.B., Averyt, M., Tignor and Miller, H.L. (Eds.). Cambridge University Press, Cambridge, United Kingdom and New York, NY, USA, pp 996.

Johnson, J.W., Nitao, J.J., Steefel, C.I., Knauss, K.G., 2001. Reactive transport modeling of geologic CO_2 sequestration in saline aquifers: the influence of intra-aquifer shales and the relative effectiveness of structural, solubility, and mineral trapping during prograde and retrograde sequestration. First National Conference on Carbon Sequestration. May 14–17, 2001, Washington, D.C., p. 60.

Jones, D.J., Beaubien, S.E., Baubron, J.C., Cinti, D., Davis, J.R., Emery, C., Fascetti, A., Lombardi, S., Michel, K., Morgantini, N., Penner, L., Quattrocchi, F., Strutt, M.H., 2006. Continued Soil Gas Monitoring at the Weyburn Unit in 2004. Report No. COAL R288 DTI/Pub URN 05/1261, p. 20.

Please cite this article as: Cantucci, B., et al., Geochemical modeling of CO_2 storage in deep reservoirs: The Weyburn Project (Canada) case study, Chemical Geology (2009), doi:10.1016/j.chemgeo.2008.12.029

Kervévan, C., Azaroual, M., Durst, P., 2005. Improvement of the calculation accuracy of acid gas solubility in deep reservoir brines: application to the geological storage of CO_2. Oil & Gas Science and Technology – Rev. IFP 60 (2), 357–379.

Kharaka, Y.K., Hanor, J.S., 2004. Deep fluids in the continents: I. Sedimentary basins. In: Holland, H.D., Turekian, K.K. (Eds.), Treatise on Geochemistry Volume 5, Surface and Ground Water, Weathering, and Soils. Elsevier-Pergamon, Oxford, UK, pp. 314–420.

Kharaka, Y.K., Cole, Hovorka, S., Gunter, W.D., Knauss, K.G., Freifeld, B.M., 2006. Gas–Water–Rock Interaction in Frio Formation Following CO_2 Injection: Implication for the Storage of Greenhouse Gases in Sedimentary Basins, vol. 34 (7). Geological Society of America, pp. 577–580.

Lagache, M., 1976. New data on the kinetics of the dissolution of alkali feldspars at 200 °C in CO_2 charged water. Geochimica et Cosmochimica Acta 40, 157–161.

Lasaga, A.C., 1984. Chemical kinetics of water–rock interactions. Journal of Geophysical Research 89, 4009–4025.

Lasaga, A.C., Soler, J.M., Ganor, J., Burch, T.E., Nagy, K.L., 1994. Chemical weathering rate laws and global geochemical cycles. Geochimica et Cosmochimica Acta 58, 2361–2386.

Lundegard, P.D., Land, L.S., 1986. Carbon dioxide and organic acids: their origin and role in diagenesis, the Texas Gulf Coast Tertiary. In: Gautier, D.L. (Ed.), Relationship of Organic Matter and Mineral Diagenesis. Society of Economic Paleontologists and Mineralogists Special Publication, vol. 38. Geological Society of America, Tulsa, OK, pp. 129–146.

Manley, E.P., Evans, L.J., 1986. Dissolution of feldspars by low molecular-weight aliphatic and aromatic acids. Soil Science 141, 106–112.

Marini, L., 2007. Geological Sequestration of Carbon Dioxide: Thermodynamics, Kinetics and Reaction Path Modeling. Elsevier XV, Amsterdam, p. 453.

Marini, L., Bonaria, V., Guidi, M., Hunziker, J.C., Ottonello, G., Vetuschi Zuccolini, M., 2000. Fluid geochemistry of the Aqui Terme-Visone geothermal area (Piemonte, Italy). Applied Geochemistry 15, 917–935.

Marini, L., Yock Fung, A., Sanchez, E., 2003. Use of reaction path modeling to identify the processes governing the generation of neutral Na–Cl and acidic Na–Cl–SO_4 deep geothermal liquids at Miravalles geothermal system, Costa Rica. Journal of Volcanology and Geothermal Research 128, 363–387.

McKibben, M.A., Barnes, H.L., 1986. Oxidation of pyrite in low temperature acidic solutions: Rate laws and surface textures. Geochimica et Cosmochimica Acta 50, 1509–1520.

Merino, E., 1979. Internal consistency of a water analysis and uncertainty of the calculated distribution of species at 25 °C. Geochimica et Cosmochimica Acta 43, 1533–1542.

Michard, G., Fouillac, C., Grimaud, D., Dennis, J., 1981. Une méthode globale d'estimation des températures des réservoirs alimentant les sources thermales. Exemple du Massif Central Français. Geochimica et Cosmochimica Acta 45, 1199–1207.

Moore, J., Adams, M., Allis, R., Lutz, S., Rauzi, S., 2005. Mineralogical and geochemical consequences of the long-term presence of CO_2 in natural reservoirs: an example from Springerville-St. Johns Field, Arizona, and New Mexico, USA. Chemical Geology 217, 365–385.

Mundy, D.J.C., Roulston, P.E., 1998. Diagenesis and porosity development of a subcropped Mississippian carbonate oil reservoir, an example from the Alida Beds of the Pheasant Rump Pool, southeast Saskatchewan. In: Christopher, J.E., Gilboy, C.F., Paterson, D.F., Bend, S.F. (Eds.), Eighth International Williston Basin Symposium. Saskatchewan Geological Society Special Publication, vol.13, pp. 86–102.

Navarre-Sitchler, A., Brantley, S., 2007. Basalt weathering across scales. Earth and Planetary Science Letters 261, 321–334.

Nordstrom, D.K., Plummer, L.N., Langmuir, D., Busenberg, E., May, H.M., Jones, B.F., Parkhurst, D.L., 1990. Revised chemical equilibrium data for major water–mineral reactions and their limitations. In: Bassett, R.L., Melchior, D. (Eds.), Chemical Modeling in Aqueous Systems II: Washington D.C. American Chemical Society Symposium Series, vol. 416, pp. 398–413. Chapt. 31.

Palandri, J.L., Kharaka, Y.K., 2004. A compilation of rate parameters of water–mineral interaction kinetics for application to geochemical modeling. U.S. Geological Survey Open File Report 2004–1068, p. 74.

Palandri, J.L., Reed, M.H., 2001. Reconstruction of in situ composition of sedimentary formation waters. Geochimica et Cosmochimica Acta 65, 1741–1767.

Palmer, D.A., Bénézeth, P., Wesolowski, D.J., 2001. Aqueous high-temperature solubility studies. I. The solubility of boehmite as functions ofionic strength (to 5 molal, NaCl), temperature (100 –290 °C), and pH as determined by in situ measurements. Geochimica et Cosmochimica Acta 65 (13), 2081–2095.

Pang, Z., Reed, M.H., 1998. Theoretical chemical thermometry on geothermal waters: problems and methods. Geochimica et Cosmochimica Acta 62, 1082–1091.

Parker, V.B., Wagman, D.D., Evans, W.H., 1971. Selected values of chemical thermodynamic properties. Tables for the alkaline earth elements (Elements 92 through 97 in the standard order of arrangement). U.S. National Bureau of Standards and Technology Note 270-6, p. 106.

Pearce, J., Springer, N., 2001. A mineralogical review of the Midale Beds (Mississippian) from the Weyburn Oilfield, south-eastern Saskatchewan. British Geological Survey Commercial Report, CR/01/146, p. 18.

Perez, R.J., Shevalier, M., Hutcheon, I., Mayer, B., 2006. A model for partitioning gases among brines and hydrocarbons in oil reservoirs: examples from the IEA–GHG Weyburn CO_2 Monitoring and Storage Project, Saskatchewan, Canada. Journal of Geochemical Exploration 89, 326–330.

Pitzer, K.S., 1973. Thermodynamics of electrolytes – I. Theoretical basis and general equations. Journal of Physical Chemistry 77, 268–277.

Pitzer, K.S., 1979. Theory: ion interaction approach. In: Pytkowicz, R.M. (Ed.), Activity Coefficients in Electrolyte Solutions. CRC Press, Boca Raton, Florida, pp. 157–208.

Pruess, K., García, J., 2002. Multiphase flow dynamics during CO_2 injection into saline aquifers. Environmental Geology 42, 282–295.

Quattrocchi, F., Bencini, R., Amorino, B., Basili, R., Caddeo, G., Cantucci, B., Cara, R., Cauli, G., Cinti, D., Deidda, C., Deriu, G., Fadda, A., Fadda, M., Fandiño, V., Ferenzena, S., Giannelli, A., Galli, G., Mazzotti, M., Ottiger, S., Pizzino, L., Pini, R., Sardu, G., Storti, G., Voltattorni, N., 2006a. Feasibility study (I stage) of CO_2 geological storage by ECBM techniques in the Sulcis Coal Province (SW Sardinia). Proceedings VIII Inter. Conf. "Green House Gases Control Technologies" (GHGT-8), Trondheim, Norway, 19–22 June 2006, pp. 223–225.

Quattrocchi, F., Barbieri, M., Bencini, R., Cinti, D., Durocher, K., Galli, G., Pizzino, L., Shevalier, M., Voltattorni, N., 2006b. Strontium isotope ($^{87}Sr/^{86}Sr$) chemistry in produced oilfield waters: the IEA Weyburn CO_2 monitoring and storage project. In: Lombardi, S., Altunina, K.L., Beaubien, S.E. (Eds.), Advances in Geological Storage of Carbon Dioxide. NATO Science Series. Springer Publishing, Berlin, pp. 243–259.

Rafal'skiy, R.P., Prisyagina, N.I., 1991. Reaction of andesine with hot aqueous solutions. Geochemistry International 28, 72–81.

Reed, M.H., Spycher, N.F., 1984. Calculation of pH and mineral equilibria in hydrothermal waters with application to geothermometry and studies of boiling and dilution. Geochimica et Cosmochimica Acta 48, 1479–1492.

Riding, J.B., Rochelle, C.A., 2004. The IEA Weyburn CO_2 monitoring and storage project. Final report of the European research team. Report No. COAL R275DTI/PubURN 05/513. British Geological Survey, Keyworth, Nottingham NG12 5GG, UK.

Robie, R.A., 1965. Heats and free energies of formation of troilite, herzenbergite, magnesite, and rhodochrosite calculated from equilibrium data. U.S. Geological Survey Professional Paper, 525-D, pp. 65–72.

Robie, R.A., Hemingway, B.S., 1977. Measurement on the enthalpy of formation of dolomite. Unpublished data.

Robie, R.A., Hemingway, B.S., 1995. Thermodynamic properties of minerals and related substances at 298.15°K and 1 bar (10^5 Pascals) and at higher temperatures. U.S. Geol. Surv. Bull., vol. 2131. U.S. Geological Survey, Reston, VA.

Robie, R.A., Hemingway, B.S., Fisher, J.R., 1979. Thermodynamic properties of minerals and relates substances at 298.15 K and 1 bar (10^5 Pascal) pressure and at higher temperatures. U.S. Geological Survey Bulletin, vol. 1452.

Rochelle, C.A., Birchall, D.J., Bateman, K., 2002. Geochemical interaction between supercritical CO_2 and the Midale formation. I: introduction to fluid–rock interaction experiments. British Geological Survey Commissioned Report Cr/02/289, p. 29.

Rutqvist, J., Tsang, C.-F., 2002. A study of caprock hydromechanical changes associated with CO_2 injection into a brine aquifer. Environmental Geology 42, 296–305.

Seewald, J.S., 2001. Model for the origin of carboxylic acids in basinal brines. Geochimica et Cosmochimica Acta 65, 3779–3789.

Sherman, L.A., Barak, P., 2000. The solubility and dissolution kinetics of dolomite ($CaMg(CO_3)_2$) in Ca–Mg–HCO_3/CO_3 solutions at 25 °C and 0.1 MPa carbon dioxide. Soil Science Society of America Journal 64, 1959–1968.

Springer, N., Stentoft, N., Fries, K., Lindgreen, H., Voigt, B., 2002. The Weyburn CO_2 monitoring project, core analysis. Danmarks og Grønlands Geologiske Undersøgelse Rapport, vol. 111, p. 71.

Spycher, N.F., Reed, M.H., 1988. Fugacity coefficients of H_2, CO_2, CH_4, H_2O and H_2O–CO_2–CH_4 mixtures: a virial equation treatment for moderate pressures and temperatures applicable to calculations of hydrothermal boiling. Geochimica et Cosmochimica Acta 52, 739–749.

Steefel, C.I., Lasaga, A.C., 1994. A coupled model for transport of multiple chemical species and kinetic precipitation/dissolution reactions with application to reactive flow in single phase hydrothermal systems. American Journal of Science 294, 529–592.

Surdam, R.C., Crossey, L.J., Hagen, E.S., Heasler, H.P., 1989. Organic–inorganic interaction and sandstone diagenesis. AAPG Bulletin 73, 1–23.

Sverdrup, H.U., 1990. The Kinetics of Base Cation Release Due to Chemical Weathering. Lund University Press, Lund, p. 246.

Teng, H.H., Fenter, P., Cheng, L., Sturchio, N.C., 2001. Resolving orthoclase dissolution processes with atomic force microscopy and X-ray reflectivity. Geochimica et Cosmochimica Acta 65, 3459–3474.

Tian, S., Zhao, G., Asghari, K., 2004. CO_2 storage during EOR process in the Weyburn oil pool: modeling and monitoring results. Proc. 7th Int. Conf. on Greenhouse Gas Control Technologies. Peer-Reviewed Papers and Plenary Presentations, vol. 1, pp. 371–379. BC, September 5–9.

Velbel, M.A., 1984. Weathering processes of rock-forming minerals. Mineral. Assoc. of Canada Short Course Handbook, vol. 10, pp. 67–111.

Velbel, M.A., 1986. Influence of surface area, surface characteristics, and solution composition on feldspar weathering rates. In: Davis, J.A., Hayes, K.F. (Eds.), Geochemical Processes at Mineral Surfaces. ACS Symposium Series, vol. 323.

Voltattorni, N., Caramanna, G., Cinti, D., Galli, G., Pizzino, L., Quattrocchi, F., 2006. Study of CO_2 natural emissions in different Italian geological scenarios: refinement of natural hazard and risk assessment. In: Lombardi, S., Altunina, K.L., Beaubien, S.E. (Eds.), Advances in Geological Storage of Carbon Dioxide. NATO Science Series. Springer Publishing, Berlin, pp. 175–190.

Wagman, D.D., Evans, W.H., Parker, V.B., Halow, I., Bailey, S.M., Schumm, R.H., 1968. Selected values of chemical thermodynamic properties. Tables for the first thirty-four elements in the standard order of arrangement. U.S. National Bureau of Standards and Technology Note 270-3, p. 264.

~~Wagman, D.D., Evans, W.H., Parker, V.B., Schumm, R.H., 1976. Chemical thermodynamic properties of compounds of sodium, potassium and rubidium: an interim tabulation of selected values. U.S. National Bureau of Standards, Interim Report 70-1034.~~

Wang, M.K., White, J.L., Hem, S.L., 1983. Influence of acetate, oxalate, and citrate anions on precipitation of aluminium hydroxide. Clays and Clay Minerals 31, 65–68.

Wegelin, A., 1984. Geology and reservoir properties of the Weyburn field, southeastern Saskatchewan. In: Lorsong, J.A., Wilson, M.A. (Eds.), Oil and Gas in Saskatchewan. Geological Society, Special Publication, vol. 7, pp. 71–82. Saskatchewan.

Please cite this article as: Cantucci, B., et al., Geochemical modeling of CO_2 storage in deep reservoirs: The Weyburn Project (Canada) case study, Chemical Geology (2009), doi:10.1016/j.chemgeo.2008.12.029

Willey, L.M., Kharaka, Y.K., Presser, T.S., Rapp, J.B., Barnes, I., 1975. Short chain aliphatic acid anions in oil field waters and their contribution to measured alkalinity. Geochimica et Cosmochimica Acta 39, 1707–1711.

Wilson, M.J., 1975. Chemical weathering of some primary rock forming minerals. Soil Science 119, 349–355.

Wilson, M., Monea, M., 2004. IEA GHG Weyburn CO_2 Monitoring & Storage Project. Summary Report 2000–2004. Petroleum Technology Research Centre, Regina, Canada, p. 273.

Wolery, T.J., 1992. EQ3NR, A Computer Program for Geochemical Aqueous Speciation-solubility Calculations: Theoretical Manual, User's Guide, and Related Documentation (version 7.0). Lawrence Livermore National Lab, Berkeley, CA, p. 246.

Xu, T., Apps, J.A., Pruess, K., 2003. Reactive geochemical transport simulation to study mineral trapping for CO_2 disposal in deep arenaceous formations. Journal of Geophysical Research 108 (B2), 2071–2084.

Xu, T., Apps, J.A., Pruess, K., 2004. Numerical simulation of CO_2 disposal by mineral trapping in deep aquifers. Applied Geochemistry 19, 917–936.

Xu, T., Apps, J.A., Pruess, K., Yamamoto, H., 2007. Numerical modeling of injection and mineral trapping of CO_2 with H_2S and SO_2 in a sandstone formation. Chemical Geology 242, 319–346.

Zerai, B., Saylor, B.Z., Matisoff, G., 2006. Computer simulation of CO_2 trapped through mineral precipitation in the Rose Run Sandstone, Ohio. Applied Geochemistry 21, 223–240.

Please cite this article as: Cantucci, B., et al., Geochemical modeling of CO_2 storage in deep reservoirs: The Weyburn Project (Canada) case study, Chemical Geology (2009), doi:10.1016/j.chemgeo.2008.12.029